Ocean Sci. Discuss., https://doi.org/10.5194/os-2017-78
Manuscript under review for journal Ocean Sci.
Discussion started: 7 November 2017

Ocean Science Discussions
Open Access
EGU

Forecasting experiments of a dynamical-statistical model of the sea surface temperature anomaly field based on the improved self-memorization principle

Mei Hong[1,2], Xi Chen[1], Ren Zhang[1,2], Dong Wang[3], Shuanghe Shen[2], and Vijay P. Singh[4]

[1]*Institute of Meteorology and Oceanography, National University of Defense Technology, Nanjing 211101, China*

[2]*Collaborative Innovation Center on Forecast and Evaluation of Meteorological Disaster, Nanjing University of Information Science &Technology, Nanjing 210044, China*

[3]*Key Laboratory of Surficial Geochemistry, Ministry of Education; Department of Hydrosciences, School of Earth Sciences and Engineering, Collaborative Innovation Center of South China Sea Studies, State Key Laboratory of Pollution Control and Resource Reuse, Nanjing University, Nanjing 210093, China*

[4]*Department of Biological and Agricultural Engineering, Zachry Department of Civil Engineering, Texas A & M University, College Station, TX 77843, USA*

Corresponding authors address:

1. Xi Chen, Research Centre of Ocean Environment Numerical Simulation, Institute of Meteorology and Oceanography, National University of Defense Technology, Nanjing 211101, China

E-mail: chenxigfkd@163.com

2. Ren Zhang, Research Centre of Ocean Environment Numerical Simulation, Institute of Meteorology and Oceanography, National University of Defense Technology, Nanjing 211101, China

E-mail: 254247175@qq.com

Ocean Sci. Discuss., https://doi.org/10.5194/os-2017-78
Manuscript under review for journal Ocean Sci.
Discussion started: 7 November 2017

Abstract: With the objective of tackling the problem of inaccurate long-term El Niño Southern Oscillation (ENSO) forecasts, this paper develops a new dynamical-statistical forecast model of sea surface temperature anomaly (SSTA) field. To avoid single initial prediction values, a self-memorization principle is introduced to improve the dynamic reconstruction model, thus making the model more appropriate for describing such chaotic systems as ENSO events. The improved dynamical-statistical model of the SSTA field is used to predict SSTA in the equatorial eastern Pacific and during El Niño and La Niña events. The long-term step-by-step forecast results and cross-validated retroactive hindcast results of time series T_1 and T_2 are found to be satisfactory, with a correlation coefficient of approximately 0.80 and a mean absolute percentage error of less than 15%. The corresponding forecast SSTA field is accurate in that not only is the forecast shape similar to the actual field, but the contour lines are essentially the same. This model can also be used to forecast the ENSO index. The correlation coefficient is 0.8062, and the MAPE value of 19.55% is small. The difference between forecast results in summer and those in winter is not high, indicating that the improved model can overcome the spring predictability barrier to some extent. Compared with six mature models published previously, the present model has an advantage in prediction precision and length, and is a novel exploration of the ENSO forecast method.

Keywords: Dynamical-statistical forecast model; self-memorization principle; sea surface temperature field; long-term forecast of ENSO

Ocean Sci. Discuss., https://doi.org/10.5194/os-2017-78
Manuscript under review for journal Ocean Sci.
Discussion started: 7 November 2017

Ocean Science Discussions
Open Access

1. Introduction

The El Niño Southern Oscillation (ENSO), the well-known coupled atmosphere –ocean phenomenon, was firstly proposed by Bjerknes (1969). The ENSO phenomenon can influences regional and global climates, so the prediction of ENSO has received considerable public interest (Rasmusson and Carpenter, 1982; Glantz et al., 1991).

Over the past two to three decades, one might reasonably expect the ability to predict warm and cold episodes of ENSO at short and intermediate lead times to have gradually improved (Barnston et al., 2012). Many countries have been focusing on ENSO forecasts since the 1990s, and the ENSO forecast has become one of the important research topics in the International Climate Change and Predictability Research plan. The U.S. International Research Institute for Climate and Society, the U.S. Climate Prediction Centre, Japan Meteorological Agency, and European Centre for Medium-Range Weather Forecasting have developed different coupled atmosphere–ocean models to forecast ENSO (Saha et al., 2006; Molteni et al., 2007) .

The forecast models can generally be divided into two types (Palmer et al., 2004). The first type is typified by a dynamic model, which mathematically expresses physical laws that govern how the ocean and the atmosphere interact. The second type is typified by a statistical model, which requires large a amount of historical data and analyses the data to do forecasting (Chen et al., 1995; Moore et al., 2006).

Over the past three decades, ENSO predictions have made remarkable progress, reaching a stage where reasonable statistical and numerical forecasts (Jin et al., 2008)can be made 6–12 months in advance (Wang et al., 2009). . However, there are three problems remaining to be resolved (Zhang et al., 2003a): (1) The current ENSO predictions are mainly limited to the short term, such as annual and seasonal predictions; (2) Although the representation of ENSO in coupled models has advanced considerably during the last decade, several aspects of the simulated climatology and ENSO are not well reproduced by the current generation of coupled models. The systematic errors in SST are often very large in the equatorial Pacific, and model representations of ENSO variability are often weak and/or incorrectly located (Neelinet al. 1992; Mechoso et al. 1995; Delecluse et al. 1998; Davey et al. 2002). (3) Coupled models of ENSO predictions initialized from observed initial states tend to adjust towards their own climatological mean and variability, leading to forecast errors. The errors associated with such adjustments tend to be more pronounced during boreal spring, which is often called the ‘‘spring predictability barrier’’ (Webster et al., 1999). More efficient models are therefore desired (Belkin and Niyogi, 2003; Weinberger and Saul, 2006). Therefore, the idea of combining dynamical and statistical methods to improve weather and climate prediction has been developed in many studies (Chou, 1974; Huang et al., 1993;Yu et al., 2014a; Yu et al.,2014b). By introducing genetic algorithms (GAs), Zhang et al. (2006) inverted and reconstructed a new dynamical-statistical forecast model of the tropical Pacific sea surface temperature (SST) field using historic statistical data (Zhang et al., 2008). However, there is one flaw in the forecast model: the time-delayed SST field. This is because ENSO is a complicated system with many influencing factors. To overcome

Ocean Sci. Discuss., https://doi.org/10.5194/os-2017-78
Manuscript under review for journal Ocean Sci.
Discussion started: 7 November 2017

information insufficiency in the forecast model, Hong et al. (2014) selected the tropical Pacific SST, SSW and SLP fields as three modelling factors and utilized the GA to optimize model parameters.

However, the above dynamical prediction equations which were ,proposed by Hong et al.(2014), greatly depend on a single initial value, creating long-term forecasts over 8 months that diverged significantly. These unsatisfactory results indicate that this model needs to be improved. Cao (1993) first proposed the self-memorization principle, which transforms the dynamical equations with the self-memorization equations, wherein the observation data can determine the memory coefficients. This method has been widely used in forecast problems in environmental, hydrological and meteorological fields (Feng et al., 2001; Gu, 1998; Chen et al., 2009). The method can avoid the question of initial conditions for the differential equations, so it can be introduced here to improve the proposed dynamical forecast model.

Therefore, an improved dynamical-statistical forecast model of the SST field and its impact factors with a self-memorization function was developed. The improved model can absorb the information from past observations.

This paper is organized as follows: Research data and forecast factors are introduced in section 2. In Section 3 the reconstruction of the dynamical model of SSTA field is described. To improve the reconstruction model, the self-memorization principle is introduced in Section 4. Model forecast experiments are described in Section 5, and conclusions are given in Section 6.

Ocean Sci. Discuss., https://doi.org/10.5194/os-2017-78
Manuscript under review for journal Ocean Sci.
Discussion started: 7 November 2017

2. Research data and forecast factors

2.1 Data

The monthly average SST data from January 1951 to January 2010, 720 months in total, were obtained from the UK Met Office Hadley Centre for the region (30°S-30°N； 120°E -90°W). The sea areas provide important information on ocean-atmosphere coupling in the East and West Pacific Ocean and the El Niño and La Niña events. The reanalysis data and zonal winds were obtained from the National Center for Environmental Forecast (NECP) of America and the National Center for Atmospheric Research (NCAR) (Kalnay et al., 1996). The SOI data were obtained from the Climate Prediction Center (CPC). The time series of all data were from Jan. 1951 to Jan. 2010.

2.2 EOF deconstruction

The sea surface temperature anomaly (SSTA) field can be calculated from the SST field and can be deconstructed into time (coefficients)-space (structure) using the EOF method. Detailed information on the EOF method can be seen in the related references (Dommenget & Latif, 2002).

An empirical orthogonal function (EOF) analysis of smoothed anomalies was performed, and the first two SSTA EOFs are shown in Figs. 1a and 1c. The principal component (PC) time series corresponding to the first and second EOFs are shown in Figs. 1b and 1d. The first EOF pattern, which accounted for 61.33% of the total SSTA variance, represented the mature ENSO phase (El Niño or La Niña), and the corresponding PC time series was highly correlated (with a correlation coefficient of

Ocean Sci. Discuss., https://doi.org/10.5194/os-2017-78
Manuscript under review for journal Ocean Sci.
Discussion started: 7 November 2017

0.85) with the cold tongue index (SST anomaly averaged over 4 °S–4 °N, 180°–90 °W) over the whole period. The second EOF, accounting for 14.52% of the total SSTA variance, indicated the ENSO signal beginning to decay. Compared with the first mode, these were slightly attenuated in terms of the scope and intensity. The above analysis is similar to the EOF analysis of the SSTA field in the previous studies (Johnson et al., 2000;Timmermann et al., 2001). This indicates that the front two variance contribution modes can describe the main characteristics of the SSTA field and El Niño/La Niña. Therefore, we can choose the T_1,T_2 time series EOF decomposition modes as the modelling objects.

2.3 Selection of other prediction model factors

The ENSO intensity impact factor is an important issue in the ENSO prediction. Previous studies have found that teleconnection patterns, temperature, precipitation, wind and SSH may affect the ENSO strength (Trenberth et al.,1998; Webster,1999; Ashok et al., 2001; Yoon and Yeh, 2010; Tomita and Yasunari, 1996). For example, Trenberth et al. (1998) noted that the Pacific North American Oscillation Index (PNA) and SOI in the Pacific Intertropical Convergence Zone (ITCZ) were all closely related to ENSO. Liao et al. (2007) also noted that the decadal variation during ENSO events had a close relationship with the SOI index.The vast majority of studies (Tomita and Yasunari, 1996; Zhou and Wu, 2010) have concentrated on the impacts of ENSO on the East Asian winter monsoon (EAWM). During the EAWM season, ENSO generally reaches its mature phase and has the most prominent impact on the climate. Wang et al. (1999a) and Wang et al. (1999b) suggested that the zonal

Ocean Sci. Discuss., https://doi.org/10.5194/os-2017-78
Manuscript under review for journal Ocean Sci.
Discussion started: 7 November 2017

wind factors in the eastern and western equatorial Pacific played a critical role in the transition phase of the ENSO cycle, which could excite eastward propagating Kelvin waves and affect the SSTA in the equatorial Pacific.

Based on the above analysis, we selected four factors, which may be closely related with the ENSO index (Niño 3.4) and were obtained as follows:

(1) The zonal wind in the eastern equatorial Pacific factor (u1) was calculated as the grid-point average of zonal wind in the area [5 °S ~ 5 °N, 150 °W ~ 90 °W].

(2) The PNA teleconnection factor was obtained from the CPC.

(3) The SOI factor was obtained from the CPC.

(4) The EAWM index (EAWMI) factor was proposed by Yang et al. (2002), which is defined by the meridional 850-hPa winds averaged over the region (20 ° ~40 °N, 100 °~140 °E).

All the four data selected ranged from January 1951 to January 2010.

Actually, how many variables and which variables are used in our model become a key issue to be resolved. We can introduce a stepwise regression principle to choose more reasonable predictors (Yim et al., 2015), because the stepwise procedure can help selecting statistically important predictors at each step. The significance of each predictor selected was based on its significance in increasing the regressed variance by the standard *F* test (Panofsky and Brier, 1968). A 95 % statistical significance level was used as a criterion to select a new predictor at each step. Once selected into the model, a predictor can only be removed if its significance level falls below 95 % by the addition/removal of another variable. For example, for

Ocean Sci. Discuss., https://doi.org/10.5194/os-2017-78
Manuscript under review for journal Ocean Sci.
Discussion started: 7 November 2017

the model of only one variable, because we forecast the ENSO index, we should choose T_1 or T_2 as the variable. Considering that T_1 accounts for 61.33% of the total SSTA variance, so we chose T_1 as the variable. For the model of two variables, there are five factors (T_2, u_1, PNA, SOI and EAWMI) which can be chosen for the second variable. Taking advantage of the stepwise regression ideas and selecting statistically important predictors by a standard F test, we can find the largest F test value among the five factors. That is T_2. Continuing this step, we can also select the reasonable factors for the model of three variables. Based on this thought, when the number of variables is determined, we can choose the most statistically important variables to reconstruct the prediction model. The forecast results of these models can be seen in table 1.

From table 1, the forecast results of all six models are satisfactory, where the temporal correlations of the models are all greater than 0.60 and the root mean square errors are all less than 0.81. Among all six models, the forecast results of four variables are the best for the following reasons:

(1) In general, the amount of parameters is less than 10% of the sample size, which can avoid over-fitting (Tetko et al., 1995) .The number of parameters $a_1, a_2, ...a_{14}, b_1, b_2, ...b_{14}, c_1, c_2, ...c_{14}, d_1, d_2, ...d_{14}$ of the model of four variables $T_1, T_2, SOI, EAWMI$ is 56, but we deleted the parameters which contributed little to the prediction. That means that there are 56 parameters in equation (1) in section 3, but there are only 34 parameters in equation (3) in section 3which is our final prediction equation. In section 5.1, because p is identified as 6, the number of parameters of the

self-memorization function β_i is 28. Therefore, the total number of parameters in the model of four variables is 62, which is less than 10% of the sample size (720 months). The number of parameters $a_1,a_2,...a_{20},b_1,b_2,...b_{20},c_1,c_2,...c_{20},d_1,d_2,...d_{20},\mathrm{e}_1,\mathrm{e}_2,...\mathrm{e}_{20}$ of the model of five variables $T_1,T_2,SOI,EAWMI,u_1$ is 100. Although the parameters which contributed a little were deleted, the number was still 72, and the number of self-memorization parameters was 30 (p determined as 5). Thus, the total number of parameters in the model of five variables was 102, which was more than 10% of the sample size (720 months).This will cause an overfitting problem. Hence, when we selected the model of five or six variables which entailed large amounts of computation that made precision difficult, and too many parameters caused an overfitting phenomenon. That is why the forecast results of five or six variables were worse than those of four variables.

(2) The models of one, two and three variables can avoid the overfitting problem, but too few variables will result in too few reconstruction parameters, causing important information missing from the model. Especially, when the model of one or two variables was considered, we only studied the self-memorization of the ENSO system but did not consider the mutual-memorization between factors. Thus, equations of our model only contained a self-memory term, not an exogenous effect term. That is why the forecast results of one, two and three variables were worse than those of four variables.

Based on the above analysis, we finally chose T_1, T_2, SOI and EAWMI as predictors for the model.

Ocean Sci. Discuss., https://doi.org/10.5194/os-2017-78
Manuscript under review for journal Ocean Sci.
Discussion started: 7 November 2017

Ocean Science Discussions
Open Access
EGU

3. Reconstruction of dynamical model based on GA

Takens' delay embedding theorem (Takens, 1981) provides the conditions under which a smooth attractor can be constructed from observations made with a generic function. Later results replaced the smooth attractor with a set of arbitrary box-counting dimensions and the class of generic functions with other classes of functions. Takens had shown that if we measured any single variable with sufficient accuracy for a long period of time, it would be possible to construct the underlying dynamical structure of the entire system from the behavior of that single variable using delay coordinates and the embedding procedure. It was therefore possible to construct a dynamical model of system evolution from the observed time series. Introducing this idea here, four time series of the T_1, T_2, SOI and EAWMI factors were chosen to construct the dynamical model.

The basic idea of statistical-dynamical model construction is discussed in Appendix A and was introduced in our previous work (Zhang et al., 2006; Hong et al., 2014).

A simplified second-order nonlinear dynamical model can be used to depict the basic characteristics of atmosphere and ocean interactions (Fraedrich, 1987). Suppose that the following nonlinear second-order ordinary differential equations are taken as the dynamical model of reconstruction. In the equations, x_1, x_2, x_3, x_4 were used to represent the time coefficient series of T_1, T_2, SOI and EAWMI.

Ocean Sci. Discuss., https://doi.org/10.5194/os-2017-78
Manuscript under review for journal Ocean Sci.
Discussion started: 7 November 2017

$$
\begin{aligned}
\frac{dx_1}{dt} &= a_1x_1 + a_2x_2 + a_3x_3 + a_4x_4 + a_5x_1^2 + a_6x_2^2 + a_7x_3^2 + a_8x_4^2 + a_9x_1x_2 + a_{10}x_1x_3 + a_{11}x_1x_4 + a_{12}x_2x_3 + a_{13}x_2x_4 + a_{14}x_3x_4 \\
\frac{dx_2}{dt} &= b_1x_1 + b_2x_2 + b_3x_3 + b_4x_4 + b_5x_1^2 + b_6x_2^2 + b_7x_3^2 + b_8x_4^2 + b_9x_1x_2 + b_{10}x_1x_3 + b_{11}x_1x_4 + b_{12}x_2x_3 + b_{13}x_2x_4 + b_{14}x_3x_4 \\
\frac{dx_3}{dt} &= c_1x_1 + c_2x_2 + c_3x_3 + c_4x_4 + c_5x_1^2 + c_6x_2^2 + c_7x_3^2 + c_8x_4^2 + c_9x_1x_2 + c_{10}x_1x_3 + c_{11}x_1x_4 + c_{12}x_2x_3 + c_{13}x_2x_4 + c_{14}x_3x_4 \\
\frac{dx_4}{dt} &= d_1x_1 + d_2x_2 + d_3x_3 + d_4x_4 + d_5x_1^2 + d_6x_2^2 + d_7x_3^2 + d_8x_4^2 + d_9x_1x_2 + d_{10}x_1x_3 + d_{11}x_1x_4 + d_{12}x_2x_3 + d_{13}x_2x_4 + d_{14}x_3x_4
\end{aligned}
\tag{1}
$$

Based on the parameter optimization search method of GA in Appendix A, the time coefficient series of T_1, T_2, SOI and EAWMI from January 1951 to April 2008 are chosen as the expected data to optimize and retrieve model parameters. To avoid the overfitting problem, we used $x_{nor} = \frac{x - x_{\min}}{x_{\max} - x_{\min}}$ to normalize the raw value of each of the four predictors, then we used the normalized value to model and forecast. Finally, we made forecast results revert back to the raw data magnitude by $x = x_{nor}(x_{\max} - x_{\min}) + x_{\min}$.

After eliminating weak items with small dimension coefficients, the nonlinear dynamical model of the first time series T_1, the second time series T_2, SOI and EAWMI can be reconstructed as follows:

$$
\begin{aligned}
\frac{dx_1}{dt} &= F_1 = -0.3328x_1 + 1.2574x_2 - 0.3511x_3 - 0.0289x_1^2 + 3.1280x_3^2 + 0.0125x_1x_2 + 2.7805x_1x_3 - 1.5408x_2x_4 \\
\frac{dx_2}{dt} &= F_2 = 1.0307x_1 - 3.1428x_2 + 0.3095x_4 + 4.2301x_1^2 - 1.2066x_2^2 + 2.5024x_4^2 - 0.2891x_1x_3 + 0.7815x_1x_4 - 0.4266x_3x_4 \\
\frac{dx_3}{dt} &= F_3 = -2.3155x_1 + 3.2166x_3 + 1.5284x_4 - 1.4527x_2^2 - 0.0034x_3^2 - 4.1206x_4^2 - 0.0025x_1x_4 + 0.0277x_2x_3 + 1.2860x_2x_4 \\
\frac{dx_4}{dt} &= F_4 = 0.4478x_2 - 0.0268x_4 + 0.8995x_1^2 - 2.3890x_3^2 + 0.2037x_4^2 + 1.3035x_1x_2 + 2.0458x_1x_4 - 2.0015x_2x_4
\end{aligned}
\tag{2}
$$

The appropriate model coefficient estimates determine the robustness of the model and the accuracy of forecast results. We should now judge whether the model coefficients are appropriate or not.

Frist, the largest Lyapunov exponent (LLE) is one of the indexes that can represent the characteristics of chaotic systems. The final Lyapunov exponents of Eq. (2) were [0.0433，0.0012，-0.1285], containing both a negative Lyapunov exponent and two positive Lyapunov exponents, which demonstrate that our dynamic system is indeed a chaotic system.

Second, we calculated the equilibrium roots of Eq. (2). Only the third equilibrium was adjudged to be stable, based upon higher-order terms within the Taylor series, the indices of which were mostly in accordance with the actual weather system. The indices in the unstable equilibria could not accurately describe the actual weather. Based on these two aspects, we can see that the model coefficient estimates were reasonable and reflected the dynamical characteristics of the model.

The model required testing. Because the training period was from January 1951 to April 2008, we chose T_1, T_2,SOI and EAWMI of May 2008, which were not used as initial forecast data in the modeling. Next, the Runge–Kutta method was used to do the numerical integration of the above equations, and every step of the integration was regarded as 1 month's worth of forecasting results. As a result, forecast results of four time series over a period of 20 months were obtained. Here, the focus was on the forecast results of T_1 and T_2, as shown in Fig.2.

From Fig. 2, forecast performance of T_1 and T_2 within 5 months was better.

Ocean Sci. Discuss., https://doi.org/10.5194/os-2017-78
Manuscript under review for journal Ocean Sci.
Discussion started: 7 November 2017

Using T_1 as an example, at this time, the temporal correlation between model predictions and corresponding observations was 0.8966 and the mean absolute percentage error (MAPE) (Hu et al., 2001), $\mathrm{MAPE}=\frac{1}{n}\sum_{i=1}^{n}\left|\frac{D_e(i)-D_0(i)}{D_0(i)}\right|\times 100$, was 8.32%. However, after 5 months, MAPE increased rapidly, and was 31.29% at 10 months. The model forecast then significantly diverged from observations, and the forecast became inaccurate. After 10 months, the forecast results became increasingly worse, which indicated that the forecast of the model after 5 months was unacceptable. The forecast results of T_2 were similar to those of T_1.

The model's skill should be further assessed by cross-validated retroactive hindcasts of the time series. As in the above example, omitting a portion of the time series (12 months, January 1951 to January 1952) from observations, we trained the model based on the data from February 1952 to December 2010, and then predicted the omitted segments (12 months, January 1951 to January 1952). We then repeated this procedure by moving the omitted segment along the entirety of the available time series. Each experiment have used the different training sample and have established the different model equation (but the method is the same).Finally, we obtained cross-validated retroactive hindcast results of T_1 and T_2, as shown in Fig. 3. Figure 3 is combined results of the 60 forecast experiments.

As Fig. 2, the forecast performance of T_1 and T_2 in Fig. 3 was not satisfactory. The model forecast significantly diverged from observations, and the forecast became inaccurate. The temporal correlations of T_1 and T_2 between model predictions and corresponding observations were 0.3411 and 0.4176, respectively. Additionally, the

Ocean Sci. Discuss., https://doi.org/10.5194/os-2017-78
Manuscript under review for journal Ocean Sci.
Discussion started: 7 November 2017

mean absolute percentage errors (MAPE) of T_1 and T_2 were 65.42% and 57.56%, respectively. This indicates that the forecast of the model in the long -term was inaccurate and unacceptable.

The forecast result may be inaccurate when the integral forecasting time is long. There will be a significant divergence which will cause an ineffective forecast. To improve the forecast accuracy, the forecast not only depends on the integral equation but also on a single initial value. Choosing the different initial value will cause different forecast accuracy. For example, in a total of 60 cross-validated retroactive hindcasts examples, the minimum MAPE was 37.65%, while the maximum MAPE was 89.88%. A forecast, depending on a single initial value, will cause instability of the forecast results. These two problems are addressed by introducing the self-memorization principle in the next section.

4. Introduction of self-memorization dynamics to improve the reconstructed model

In the above discussion, it was shown that the accuracy of the forecast results of equation (2) were unsatisfactory. To improve long-term forecasting results, the principle of self-memorization can be introduced into the mature model (Gu 1998; Chen et al., 2009). The principle of self-memorization dynamics (Cao, 1993; Feng et al., 2001) can be seen in Appendix B.

Based on Eq. (B10) in Appendix B, the improved model can be expressed as

follows:
$$\begin{cases} x_{1t} = \sum_{i=-p-1}^{-1} \alpha_{1i} y_{1i} + \sum_{i=-p}^{0} \theta_{1i} F_1(x_{1i}, x_{2i}, x_{3i}, x_{4i}) \\ x_{2t} = \sum_{i=-p-1}^{-1} \alpha_{2i} y_{2i} + \sum_{i=-p}^{0} \theta_{2i} F_2(x_{1i}, x_{2i}, x_{3i}, x_{4i}) \\ x_{3t} = \sum_{i=-p-1}^{-1} \alpha_{3i} y_{3i} + \sum_{i=-p}^{0} \theta_{3i} F_3(x_{1i}, x_{2i}, x_{3i}, x_{4i}) \\ x_{4t} = \sum_{i=-p-1}^{-1} \alpha_{4i} y_{4i} + \sum_{i=-p}^{0} \theta_{4i} F_4(x_{1i}, x_{2i}, x_{3i}, x_{4i}) \end{cases} \quad (3)$$

where y_i is replaced by the mean of two values at adjoining times; i.e., $y_i \equiv \frac{1}{2}(x_{i+1} + x_i)$; F is the dynamic core of the self-memorization equation, which can be obtained from Eq. (2); and α and θ are the memory coefficients, the formula for which can be found in Appendix B.

If the values of α and θ can be obtained, Eq. (3) can be used to obtain the results of final prediction. The memory coefficients α and θ in Eq. (3) were calibrated using the least-squares method with the same data (January 1951 to April 2008) as those used in Section 3. Eq. (3) can be deconstructed as follows (M is the length of the time series):

$$X = \begin{bmatrix} x_{11} \\ x_{12} \\ . \\ . \\ . \\ x_{1\mathrm{M}} \end{bmatrix}, \alpha = \begin{bmatrix} \alpha_{-p-1} \\ \alpha_{-p} \\ . \\ . \\ . \\ \alpha_{-1} \end{bmatrix}, Y = \begin{bmatrix} y_{-p-1,1} & y_{-p,1} & \cdots & y_{-1,1} \\ y_{-p-1,2} & y_{-p,2} & \cdots & y_{-1,2} \\ . & . & & . \\ . & . & & . \\ . & . & & . \\ y_{-p-1,\mathrm{M}} & y_{-p,\mathrm{M}} & \cdots & y_{-1,M} \end{bmatrix}, \Theta = \begin{bmatrix} \theta_{-p} \\ \theta_{-p+1} \\ . \\ . \\ . \\ \theta_0 \end{bmatrix},$$

$$F = \begin{bmatrix} F_{-p,1} & F_{-p+1,1} & \cdots & F_{0,1} \\ F_{-p,2} & F_{-p+1,2} & \cdots & F_{0,2} \\ . & . & & . \\ . & . & & . \\ . & . & & . \\ F_{-p,M} & F_{-p+1,\mathrm{M}} & \cdots & F_{0,\mathrm{M}} \end{bmatrix}$$

Ocean Sci. Discuss., https://doi.org/10.5194/os-2017-78
Manuscript under review for journal Ocean Sci.
Discussion started: 7 November 2017

The matrix equation is:

$$X = Y\alpha + F\theta \qquad (4)$$

where $Z = [Y \vdots F]$, $W = \begin{bmatrix} \alpha \\ \vdots \\ \Theta \end{bmatrix}$.

Eq. (4) can be written as:

$$X = ZW \qquad (5)$$

The memory coefficients vector W can be calibrated using the least squares method:

$$W = (Z^T Z)^{-1} Z^T X \qquad (6)$$

The memory coefficients a, θ can be obtained from Eq. (6). We then made a prediction using the self- memorization equation (3), which used the p values before t_0.

The coefficients in F and W were used with the same training data from January 1951to Apr.il 2008. In the forecast examples, we trained both the coefficients in F and W at the same time, but in the paper we describe them separately to facilitate the reader for better understanding.

5. Model prediction experiments

5.1 Forecast of time series T_1 and T_2

The training sample for the model was from January1951 to April 2008. Here, from Eq. (3), the forecast results using T_1, T_2, SOI and EAWMI factors can be calculated, called as step-by-step forecast.

When the retrospective order p is confirmed, step-by-step forecasts can be

Ocean Sci. Discuss., https://doi.org/10.5194/os-2017-78
Manuscript under review for journal Ocean Sci.
Discussion started: 7 November 2017

carried out. For example, when the T_1,T_2, SOI and EAWMI values of May 2008 were forecast, y_i was obtained from the previous $p+1$ time of T_1,T_2, the SOI and the EAWMI data, and $F_i(x_{1i},x_{2i},x_{3i},x_{4i})$ was obtained from the previous p times of T_1,T_2, the SOI and the EAWMI data. All four equations were integrated simultaneously. Taking these in Eq. (3), we can get the T_1,T_2, SOI and EAWMI values of May 2008, which these can be taken as the initial values for the next prediction step. Then, the T_1,T_2, SOI and EAWMI values from June 2008 and so on, can be generated.

5.1.1 Determination of p

Based on the self-memorization principle, the self-memorization of the system determines the retrospective order p (Cao, 1993). If the system forgets slowly, parameters a and θ will be small and the p value should be high. The SSTA field forecasts were on a monthly scale, the change of which was slow in contrast to large-scale atmospheric motion. So parameters a and θ were small, and generally, the p value was in the range 5 to 15.

The retrospective order p was obtained by a trial calculation method. We selected the p values in the range 4 to 16 to construct the model. The correlation coefficients (CC) and MAPE of long-term fitting test (from February 1951 to December 2010) are shown in Table 2, which can be used as the standard to determine the retrospective order p.

Table 2 indicates that when $p=6$, the MAPE values of long-term fitting test were the smallest and the correlation coefficients were the largest. Also, when p from 5 to 9, CCs were all more than 0.58 and the forecast results were all good, which is

Ocean Sci. Discuss., https://doi.org/10.5194/os-2017-78
Manuscript under review for journal Ocean Sci.
Discussion started: 7 November 2017

consistent with our interpretation of the physical mechanisms in section 6.2 below. SOI and EMWMI were 5-12 months lead relationships with SST (Xu et al., 1993; Chen et al, 2010; Wang et al., 2003). Using a cumulative period of SOI , EMWMI 5-8 months ahead as initial values can help improve the final forecast results. Our results in table 2 are consistent with the actual physical ENSO process. Therefore, we selected the retrospective order as *p*=6.

Then, the prediction experiments can be carried out, based on improved self-memorization Eq. (3).

The improved self-memorization equation of T_1,T_2, SOI and EAWMI can then be established. After the differential equation was discretely dealt with, the memory coefficients were solved by the least-squares method given in section 4 (Training period is January 1951 to April 2008). Finally, the improved prediction equation of T_1,T_2, SOI and EAWMI, based on the self-memorization principle, can be expressed as:

$$\begin{cases} x_{1t} = \sum_{i=-7}^{-1} \alpha_{1i} y_{1i} + \sum_{i=-6}^{0} \theta_{1i} F_1(x_{1i}, x_{2i}, x_{3i}, x_{4i}) \\ x_{2t} = \sum_{i=-7}^{-1} \alpha_{2i} y_{2i} + \sum_{i=-6}^{0} \theta_{2i} F_2(x_{1i}, x_{2i}, x_{3i}, x_{4i}) \\ x_{3t} = \sum_{i=-7}^{-1} \alpha_{3i} y_{3i} + \sum_{i=-6}^{0} \theta_{3i} F_3(x_{1i}, x_{2i}, x_{3i}, x_{4i}) \\ x_{4t} = \sum_{i=-7}^{-1} \alpha_{4i} y_{4i} + \sum_{i=-6}^{0} \theta_{4i} F_4(x_{1i}, x_{2i}, x_{3i}, x_{4i}) \end{cases} \quad (7)$$

where

Ocean Sci. Discuss., https://doi.org/10.5194/os-2017-78
Manuscript under review for journal Ocean Sci.
Discussion started: 7 November 2017

$$\alpha=[\alpha_{ij}]=\begin{bmatrix} 0.0315 & -2.113 & 0.0284 & 2.1468 & 0.0688 & -0.7014 & 1.3248 \\ 0.4088 & -1.887 & -1.0233 & 1.5485 & 0.9028 & 1.0255 & -0.6443 \\ -0.9088 & -0.2557 & 0.9671 & -0.0054 & 1.0568 & 2.9764 & -0.5234 \\ 0.2088 & -1.0567 & 0.4891 & -0.5066 & -0.4890 & 1.4555 & 1.0966 \end{bmatrix}$$

$(i=0,1,\ldots,4;\ j=-7,-6,\ldots,-1)$

$$\theta=[\theta_{ij}]=\begin{bmatrix} 0.0485 & 0.0425 & -1.7688 & 0.8543 & 2.8901 & -0.1788 & -0.9066 \\ 0.07642 & 0.0941 & -1.2466 & -0.2288 & 0.1097 & 2.3221 & -1.4228 \\ -0.5288 & 1.2368 & -0.5568 & -0.0155 & 0.2886 & -0.1560 & 1.2775 \\ 1.5335 & -0.2887 & -0.5336 & -0.6072 & -0.5611 & 1.0225 & -1.0625 \end{bmatrix}$$

$(i=0,1,\ldots,4;\ j=-6,-5,\ldots,0)$

The step-by-step forecast was performed. The retrospective order $p=6$ means that earlier seven observation data ($p+1=7$) should be used during the forecasting process. The forecast results per month were saved for the next period predictions.

5.1.2 Long-term step-by-step forecasts of T_1 and T_2

To test the actual forecast performance of the above improved model, long-term step-by-step forecasts of T_1 and T_2 from May 2008 to December 2010 for 20 months were carried out, as shown in Fig. 4. The forecast results of T_1 and T_2 were good. Within 8 months, the correlation coefficients of T_1 and T_2 were 0.9163 and 0.9187. MAPEs of T_1 and T_2 were small, only 5.86% and 6.78%. The forecast time series from 8 months to 14 months gradually diverged, but the trend was acceptable. The correlation coefficients of T_1 and T_2 reached 0.8375 and 0.8251, and MAPEs of T_1 and T_2 were 8.32% and 9.11%. After 14 months, forecast began to diverge and the error started to increase, but the correlation coefficients of T_1 and T_2 remained about 0.6899 and 0.6782, and MAPEs reached 18.31% and 19.44%, which can be acceptable.

5.2 Cross-validated retroactive hindcasts of time series T_1 and T_2

Ocean Sci. Discuss., https://doi.org/10.5194/os-2017-78
Manuscript under review for journal Ocean Sci.
Discussion started: 7 November 2017

As in section 3, the model's skill should be further assessed by cross-validated retroactive hindcasts of the time series. Because our step-by-step forecasts need the earlier seven observation data ($p+1=7$), we can obtain cross-validated retroactive hindcast results of T_1 and T_2 from August 1951 to December 2010, as shown in Fig. 5.

From Fig. 5, the forecast performance of T_1 and T_2 was good. The correlation coefficients of T_1 and T_2 were 0.7124 and 0.7036, respectively. The MAPEs of T_1 and T_2 were small, only 19.57% and 19.79%, respectively. The peaks and valleys of T_1 and T_2 were also forecasted accurately. The forecast results indicated that the cross-validated retroactive hindcast results of T_1 and T_2 were close to the observed values. Compared to Fig. 3, the improved model had better forecast abilities than the original model.

Many researchers (Zhang et al., 2003b; Smith, 2004) have used Oceanic Niño Index (ONI) which is used by the U.S. NOAA Climate Prediction Center to determine the El Niño and La Niña years. It defined that the ONIs of five consecutive months in winter were all more than 0.5 (less than -0.5) is the ElNiño (La Niña) year. Based on the above criterion, we can divide the total 60 years (1951-2010) into three categories. It includes the 18 examples of ElNiño year (such as 1958, 1964, 1966, etc.), 22 examples of LaNiña year (such as 1951, 1955, 1956, etc.) and the remaining 20 experiments of the neutral year. Since the details in Fig.5 is not clear, we list the forecast results of 60 experiments (including 18 El Niño examples, 22 La Niña examples and 20 Neutral examples) in table 3.

Ocean Sci. Discuss., https://doi.org/10.5194/os-2017-78
Manuscript under review for journal Ocean Sci.
Discussion started: 7 November 2017

From table 3, the average of CC of both T_1 and T_2 of 60 experiments within 6 months was more than 0.84 and MAPE was less than 8%. The average of CC within 12 months was more than 0.74 and MAPE was less than 12%. According to the literature (Barranel et al., 1999), when MAPE was less than 15%, which means the error was not great and the forecast results were good. Obviously, the forecast results of ElNiño / LaNiña experiments were a little worse than those of neutral examples, which means the forecast ability of our model for the abnormal situation was a little worse than those for the normal situation. But even for ElNiño / LaNiña experiments, the average of CC was still more than 0.7 and MAPE was less than 15%, which means the error was not too large and was still within an acceptable range.

5.3Forecast of the SSTA field

When we obtained the forecast results of the time coefficient series T_1 and T_2, we submitted them into the following equation to reconstruct the forecast SSTA field:

$$\hat{x}_t = \sum_{n=1}^{2} E_n \bullet T_{nt}, t = 1, 2, ..., 12 \qquad (8)$$

where E_n , T_{nt} are the EOF space fields and forecast time coefficients, respectively, and $\hat{x}_{tj}$ is the forecast SSTA field reconstructed by EOF.

After reconstruction of the space mode (treated as constant) and time coefficient series (model prediction), the forecast of the SSTA fields was obtained, based on the forecast results of T_1 and T_2 in Section 5.2. For economy of space, we cannot draw all of the forecasted SSTA fields, so we selected a strong El Niño event (December 1997), a strong La Niña event (December 1999) and a neutral event (November 2002) as examples.

Fig. 6 shows the forecast SSTA field during a strong El Niño event. From the

Ocean Sci. Discuss., https://doi.org/10.5194/os-2017-78
Manuscript under review for journal Ocean Sci.
Discussion started: 7 November 2017

actual SSTA field in December 1997 (Fig. 6a), an obvious warm tongue structure occurred in the area of [10°S～5°N，90°W～150°W] in the Eastern Equatorial Pacific, and a warm anomalous distribution arose in the west Pacific, which indicated a weak El Niño event. The forecasted SSTA field of December 1997 is shown in Fig. 6b. Although the range of warm tongue was a litter bigger than the actual situation, the forecast shape was similar to the actual field and also the contour lines were similar. The average MAPE between the forecast field and the actual field is 8.56%, which was controlled within 10%. The forecast results of the improved model event were quite good for the El Niño event.

Fig.7 shows the forecasted SSTA field of a strong La Niña event. From the actual SSTA field in December 1999 (Fig. 7a), an obvious cold pool occurred in the area of [10°S～10°N，120°W～180°W] in the Equatorial Pacific, which covered the Niño3.4 area. This SSTA field presented a strong strength La Niña event. The forecast SSTA field from December 1999 is shown as Fig. 7b. Although the strength of the cold pool was weaker than the actual situation, the forecast shape was similar to that of the actual field. The average MAPE between the forecast field and the actual field was 9.69%. The errors were larger than that of the El Niño event, but they can be controlled within 10%, which is acceptable.

Fig. 8 shows the forecasted SSTA field of a neutral event. From the actual SSTA field in November 2002 (Fig. 8a), a warm pool occurred in the area of [10°S～10°N，120°W～180°W] in the Equatorial Pacific, which covered the Niño3.4 area. However, the warm pool was small and weak, which represented a neutral event. The forecasted

Ocean Sci. Discuss., https://doi.org/10.5194/os-2017-78
Manuscript under review for journal Ocean Sci.
Discussion started: 7 November 2017

SSTA field from November 2002 is shown in Fig. 8b. Comparing Figures 6, 7 and 8, we can see that the forecasted SSTA field of a neutral event was a little worse than thatof the El Niño and La Niña events. The forecasted shape of the SSTA field basically described the actual situation, but the warm pool in the Niño3.4 area was stronger and bigger than that of the actual situation, which indicated a borderline El Niño event. The average MAPE between the forecasted field and the actual field was 14.50%, which was big but can be accepted.

We obtained the average values of MAPE of 18 El Niño events, 22 La Niña events and 20 neutral events, which were 9.52%, 9.88% and 14.67%, respectively, representing a good SSTA field forecasting ability of our model.

5.4 Forecast of ENSO index

The ENSO index can be represented as the sea surface temperature anomaly (SSTA) in the Niño-3.4 region (5 °N-5 °S, 120 °-170 °W) and the ENSO index forecast was the 3-month forecast (Barnston et al. 2012). So we also can pick up the ENSO index from the above forecasted SSTA field. The forecast results of the ENSO index within 20 months can also be obtained. The definition of lead time can be seen in the reference (Barnston et al. 2012). Therefore, similar to the forecast experiment in section 5.1, a succession of running 3-month mean SST anomalies with respect to the climatological means for the respective prediction periods, averaged over the Niño 3.4 region, can be obtained, as demonstrated in Fig. 9.

The forecast results within lead times of 18 months are shown in Fig. 9, which demonstrate that the forecast results of the ENSO index are good. Within lead time of

Ocean Sci. Discuss., https://doi.org/10.5194/os-2017-78
Manuscript under review for journal Ocean Sci.
Discussion started: 7 November 2017

12 months, the correlation coefficient was 0.8985 and the MAPE value was small, only 8.91%. In addition, the borderline La Niña event in 2008–2009 was predicted well. After lead times of 12 months, forecasts began to diverge and the errors started to increase. Although the correlation coefficient remained approximately 0.61, MAPE reached 18.58%. Therefore, a moderate strength El Niño event that occurred in 2009/10 was not predicted.

We should give more examples to test the ENSO prediction ability of our model. As in section 5.3, we can divide 60 examples as three types, which are examples of ElNiño year, LaNiña year and neutral year. Finally, we can obtain the forecast results of different types of examples in different lead times, as shown in table 4.

From table 4, the average CC of 60 experiments was 0.712 and the average MAPE was 7.62% within 12 months for all seasons of lead time, which indicates that the overall ENSO forecast ability of our model was good. The forecast results of the El Niño examples were significantly worse than those of La Niña examples, while the forecast results of La Niña examples were significantly worse than those of neutral examples, which show the model forecast ability of the abnormal state was worse than the normal state of the ENSO index. Even for the forecast results of El Niño examples, the average CC was still above 0.6 and the average MAPE can be controlled below 10%, which means the forecast results were still in the acceptable range. Our model not only accurately predicted the stronger El Niño and La Niña phases but also the neutral states. But the forecast results in summer were a little worse than those in winter, as shown in Fig.10.

Ocean Sci. Discuss., https://doi.org/10.5194/os-2017-78
Manuscript under review for journal Ocean Sci.
Discussion started: 7 November 2017

The ENSO forecast often had a spring predictability barrier (Webster, 1999), which was most prominent during decades of relatively poor predictability (Balmaseda et al., 1995).To test our model, the skill should be computed over the entire time series and separately for seasonal subsets of the time series. The average cumulative correlation coefficient and MAPE of winter were compared with those of summer, as shown in Fig.10. The average cumulative correlation and average cumulative MAPE values between the forecast values and the actual values changed with time, from which good trends of forecast results can be seen. As long as the forecast time increased, the cumulative MAPE increased and the correlation decayed gradually. The forecast results appeared to diverge. Although the forecast results of the present model in the summer were worse than in the winter, the margin was not high, which means the model can overcome the "spring predictability barrier," to some extent.

5.5 Compared with six mature models

Barnston et al. (2012) compared many ENSO forecast models. Based on his research, we selected four high quality dynamical models, including ECMWF, JMA, the National Aeronautics and Space Administration Global Modelling and Assimilation Office (NASAGMAO) and the National Centre for Environmental Prediction Climate Forecast System (NCEP CFS; Version1). Two high quality statistical models also be selected, including the University of California, Los Angeles Theoretical Climate Dynamics (UCLA-TCD) multilevel regression model and the NOAA/NCEP/CPC constructed Analogue (CA) model. The detail of the above models can be seen in these references (Reynoldset al., 2002; Luo et al., 2005; Barnston et al., 2012).

We then compared the forecast ability of the above six models with that of our mode. All of the experiments of our model and six other models were conducted under the same conditions using the same historical data for modelling and the same initial values to forecast. In the CPC website, there are detailed explanations of six models' training samples and the initial values. So we do not need to install all these models on their own machines and run them for forecasting. We just made training samples and initial values of our model were the same with those of selected six models. At an 8-month lead time, the correlation ability of our model for all seasons combined was 0.613 (Fig. 11). In brief, the forecast ability of the ECMWF model was slightly better than that of our model but the ability of the other 5 models was worse than that of our model. While, in regard to the forecast length, the temporal correlation within 12 months of our model is greater than 0.6, which was superior to the ECMWF model. In addition, the forecast results of the UCLA-TCD model and the CPC CA model reduced quickly after 5-month lead times, so the forecast ability of our model was more stable than them.

The root mean square error (RMSE) was also examined to assess the performance of discrimination and calibration. Barnston et al. (2012) believed that all seasonal RMSE values contributed equally to a seasonally combined RMSE. So we drew figure 12 to show seasonally combined RMSE.

From Fig. 11 and Fig. 12, we can see the highest correlation tend to have

Ocean Sci. Discuss., https://doi.org/10.5194/os-2017-78
Manuscript under review for journal Ocean Sci.
Discussion started: 7 November 2017

lower RMSE. So the RMSE of our model was slightly higher than that of ECMWF model, but it was much lower than those of the other 5 models.

6. Conclusions and discussion

6.1 Conclusions

A new forecasting model of the SSTA field was proposed based on a dynamic system reconstruction idea and the principle of self-memorization. The approach of the present paper consisted of the following steps:

(1) The SST field can be time (coefficients)-space (structure) deconstructed using the EOF method. Take T_1, T_2, SOI and EAWMI and consider them as trajectories of a set of four coupled quadratic differential equations based on the dynamic system reconstruction idea. The parameters of this dynamic model were estimated using a GA.

(2) The forecast results of the dynamic model can be improved by the self-memorization principle. The memory coefficients in the improved self-memorization model were obtained using the GA method.

(3) The long-term step-by-step forecast results and cross-validated retroactive hindcast results of time series T_1 and T_2 are all found to be good, with a correlation coefficient of approximately 0.80 and a mean absolute percentage error of less than 15%.

(4) The improved model was used to forecast the SSTA field. The forecasted SSTA fields of three types of events are accurate. Not only is the forecast shape similar to the actual field but also the contour lines are similar.

Ocean Sci. Discuss., https://doi.org/10.5194/os-2017-78
Manuscript under review for journal Ocean Sci.
Discussion started: 7 November 2017

(5) The improved model was also used to forecast the ENSO index. The average correlation coefficient of 60 examples within 12 months is 0.712, and the MAPE value is small, only 7.62%, which proves that the improved model has better forecasting results of the ENSO index. Although the forecast results of the model in the summer were worse than in the winter, the margin was not high, which means that the model can overcome the spring predictability barrier to some extent. Finally, compared with the six mature models, the new dynamical-statistical forecasting model has a scientific significance and practical value for the SST in the eastern equatorial Pacific and El Niño/La Niña event predictions.

6.2 Discussion

Because the formula of our model includes a linear combination of 4 variables (t_1, t_2, SOI, EAWM), statistical forecasting requires independence between predictors. We can calculate the correlation coefficients between variables, as shown in table 5. In fact, as Table 5 shows, the correlation coefficients between the factors were all less than 0.45, indicating the independence between factors. So this does not generate too much redundancy and can avoid an overfitting problem, which can destroy the stability of the model.

The introduction of self-memorization essentially introduces a lot of new coefficients, which may cause an overfitting problem. Because we have selected a model of four variables, there is a total of 62 parameters. In order to avoid the overfitting problem, the sample sizes are more than 10% of the amount of parameters. So our sample size is greater than 620 data to avoid the overfitting problem. If we choose the model of three variables, the parameters in which will be less, the sample size in this situation can be less. But the forecast results may be a little worse, based on the analysis in section 2.3. So the length of training samples is related to the number of parameters of our model.

Also, we have tried to detrend our data before the model constructed. But we found the results didn't change too much. That is mean our model is not very sensitive to climate change, so the detrended data has little effect for our model to improve the forecast effect.

Compared with the original model, why the improved model has good forecast results and can overcome the spring predictability barrier to some extent are as follow: Recently, many studies have pointed out that spring is the most unstable season of the air - sea interaction and the error is likely to develop or grow in the spring, resulting in the spring predictability barrier (Zhang et al, 2012; Philander et al., 1992). When the original model uses the indexes in summer as the initial values to predict, the SOI factor representing the air-sea interaction is most unstable in the spring and the EMWMI factor does not have much influence on ENSO in summer, so the forecast results using the indexes in summer as the initial values are certainly much worse than those using the indexes in the winter as the initial values. That is why our original model does not overcome the spring predictability barrier.

However, the introduction of the self-memorization dynamics principle can help our model overcome the spring predictability barrier to some extent. Although the lead time is still summer (such as JJA), the information of the initial value actually

Ocean Sci. Discuss., https://doi.org/10.5194/os-2017-78
Manuscript under review for journal Ocean Sci.
Discussion started: 7 November 2017

contains the previous p + 1 month (in this case p = 6, which contains the information of the previous seven months, including the information of T_1, T_2 , SOI, EMWMI factor in winter (January, February), spring (March, April, May) and summer (June and July)). From the dynamical analysis, in this situation, the information and interaction relationship of four factors have been a long period (from winter to summer) accumulated, containing much air-sea interaction processes and winter monsoon continued abnormal information, so the forecast results of our improved model will be much better than the original model which simply uses only one initial value. That is why the improved model overcomes the spring predictability barrier to some extent.

The forecast results of our model are good, but it still has some problems:

(1) Although the reason why the improved model has good forecast results has disucussed in the section6.2, the deep physical mechanisms that the proposed model has dealt with is not very clear, so its dynamical characteristics should be further analysed.

(2)The experiments in the present study have proven that the forecasting results of the improved model are good for large-scale systems, such as ENSO events, and the forecasting period has been extended. However, for small-scale systems, such as Hurricanes, whether the forecast results could be improved using the present improved model needs to be further verified.

(3) Our paper focuses primarily on these defined indices with T_1, T_2 to reconstruct a prediction model. Maybe, we can select variables (predictor) based on

EOF analysis and our model may be a more physically oriented model. Maybe we can learn from Yim et al (2013; 2015) to draw correlation maps between these fields and the SSTA field and select the predictors from physical considerations. All these above questions require that a lot of experiments to be carried out.

These items will be our future work.

Acknowledgments This study was supported by the Chinese National Natural Science Fund (nos 41375002，41075045, 41306010, 41571017, 51190091 and 41071018) and the Chinese National Natural Science Fund (BK20161464) of Jiangsu Province, the Program for New Century Excellent Talents in University (NCET-12-0262), the China Doctoral Program of Higher Education (20120091110026), the Qing Lan Project, the Skeleton Young Teachers Program, and the Excellent Disciplines Leaders in Midlife-Youth Program of Nanjing University.

APPENDIX A: THE PRINCIPLE OF DYNAMICAL MODEL RECONSTRUCTION

Suppose that the physical law of a nonlinear system going by over time can be expressed as the following difference form:

$$\frac{q_i^{(j+1)\Delta t} - q_i^{(j-1)\Delta t}}{2\Delta t} = f_i(q_1^{j\Delta t}, q_2^{j\Delta t}, \ldots, q_i^{j\Delta t}, \ldots, q_N^{j\Delta t}) \quad j = 2,3,\ldots\ldots M-1 \qquad \text{(A1)}$$

where f_i is the generalized nonlinear function of $q_1, q_2, \ldots, q_i, \ldots, q_N$, N is the number of variables, and M is the length of observed data. $f_i(q_1^{j\Delta t}, q_2^{j\Delta t}, \ldots, q_i^{j\Delta t}, \ldots, q_N^{j\Delta t})$ can be assumed to contain two parts: G_{jk} representing the expanding items which contain variable

Ocean Sci. Discuss., https://doi.org/10.5194/os-2017-78
Manuscript under review for journal Ocean Sci.
Discussion started: 7 November 2017

q_i , P_{ik} just representing the corresponding parameters which are real numbers ($i=1,2,...N$, $j=1,2,...M$, $k=1,2,...,K$).

It can be supposed as follows:

$$f_i(q_1,q_2,...,q_n)=\sum_{k=1}^{K}G_{jk}P_{ik} \qquad \text{(A2)}$$

$D=GP$ is the matrix form of Eq.(A2) , in which

$$D=\begin{Bmatrix} d_1 \\ d_2 \\ ... \\ d_M \end{Bmatrix}=\begin{Bmatrix} \dfrac{q_i^{3\Delta t}-q_i^{\Delta t}}{2\Delta t} \\ \dfrac{q_i^{4\Delta t}-q_i^{2\Delta t}}{2\Delta t} \\ ... \\ \dfrac{q_i^{M\Delta t}-q_i^{(M-2)\Delta t}}{2\Delta t} \end{Bmatrix}, \quad G=\begin{Bmatrix} G_{11},G_{12},......G_{1K} \\ G_{21},G_{22},......G_{2,K} \\ ... \\ G_{M1},G_{M2},.....G_{M,K} \end{Bmatrix}, \quad P=\begin{Bmatrix} P_{i1} \\ P_{i2} \\ ... \\ P_{iK} \end{Bmatrix} \qquad \text{(A3)}$$

Parameters of the above equation can be determined through inverting the observed data. Vector P which satisfies the above equation can be solved, based on a given vector D. Assuming q is unknown, it is a nonlinear system. However, assuming P is unknown, it is a linear system.

With the restriction $S=(D-GP)^T(D-GP)$ as a minimum, GA is introduced as an optimization solution search in the model parameters space.

Assuming that the parameters matrix P is the population (solutions), the $S=(D-GP)^T(D-GP)$ is an objective function, $l_i=\dfrac{1}{S}$ is the value of individual fitness, and $L=\sum_{i=1}^{n}l_i$ is the value of total fitness. The operating steps of GA include: creation and coding of initial population (solutions), fitness calculation, the choice of male parents, crossover and variation, etc. A detailed theoretical explanation can be got from Wang (2001). The step length is 1 month during the calculation. After optimization searches and genetic operations, the target value can be rapidly converged on and each optimal parameter of the dynamical equations can be obtained.

Ocean Sci. Discuss., https://doi.org/10.5194/os-2017-78
Manuscript under review for journal Ocean Sci.
Discussion started: 7 November 2017

Through the above approach, we can obtain parameters of a nonlinear dynamical system, and reconstruct the nonlinear dynamical equations from observed data.

APPENDIX B: THE MATHEMATICAL PRINCIPLE OF SELF-MEMORIZATION DYNAMICS OF SYSTEMS

The dynamical equations of a system can be expressed as:

$$\frac{\partial x_i}{\partial t} = F_i(x, \lambda, t) \quad i = 1, 2, ..., J \qquad \text{(B1)}$$

where J is an integer， x_i is the ith variable of the system state, and λ is the parameter. Equation (B1) represents the relationship between a source function F and a local change of x . Obviously, x is a scalar function with time t and space r_0 . A set of time $T = [t_{-p} ... t_0 ... t_q]$ can be considered, where t_0 is an initial time. A set of space $R = [r_a ... r_i ... r_\beta]$ can be considered, where r_i is a spatial point. An inner product in space $L^2 : T \times R$ is defined by:

$$(f, g) = \int_a^b f(\xi) g(\xi) d\xi, \; f, g \in L^2 \qquad \text{(B2)}$$

Accordingly, a norm can be defined as:

$$\| f \| = [\int_a^b (f(\xi)^2 d\xi]^{1/2}$$

For a completion L^2 , it can become a Hilbert space H . A generalized one in H can be regarded as a solution of the multi-time model. By introducing a memorization function $\beta(r, t)$, we can obtain:

Ocean Sci. Discuss., https://doi.org/10.5194/os-2017-78
Manuscript under review for journal Ocean Sci.
Discussion started: 7 November 2017

$$\int_{t_0}^{t} \beta(\tau)\frac{\partial x}{\partial \tau}d\tau = \int_{t_0}^{t} \beta(\tau)F(x,\tau)d\tau \qquad \text{(B3)}$$

where r in $\beta(r,t)$ can be dropped through fixing on the spatial point r_0. Suppose that function $\beta(r,t)$ and variable x etc. are all continuous, differentiable and integrable, an integration by the left parts of Eq. (B3) can be made as:

$$\int_{t_0}^{t} \beta(\tau)\frac{\partial x}{\partial \tau}d\tau = \beta(t)x(t) - \beta(t_0)x(t_0) - \int_{t_0}^{t} x(\tau)\beta'(\tau)d\tau \qquad \text{(B4)}$$

where $\beta'(t) = \partial\beta(t)/\partial t$. The mean value theorem can be introduced into the third term in Eq. (B4), the following equation can be obtained:

$$-\int_{t_0}^{t} x(\tau)\beta'(\tau)d\tau = -x^m(t_0)[\beta(t) - \beta(t_0)] \qquad \text{(B5)}$$

where $x^m(t_0) \equiv x(t_m), t_0 < t_m < t$. Substituting Eq. (B4) and Eq. (B5) in Eq. (B3) and carrying out an algebraic operation, the following equation can be obtained:

$$x(t) = \frac{\beta(t_0)}{\beta(t)}x(t_0) + \frac{\beta(t) - \beta(t_0)}{\beta(t)}x^m(t_0) + \frac{1}{\beta(t)}\int_{t_0}^{t} \beta(\tau)F(x,\tau)d\tau \qquad \text{(B6)}$$

Because the x value which is at initial time t_0 and middle time t_m, only on the fixed point r_0 itself , relates to the first term and the second term in Eq. (B6) , they are be called as a self-memory term. Also, we can call the third term as an exogenous effect, i.e., which is contributed by other spatial points.

Similarly as Eq. (B4), for multi-time t_i, $i = -p, -p+1 \ldots, t_0, t$, it gives

$$\int_{t_{-p}}^{t_{-p+1}} \beta(\tau)\frac{\partial x}{\partial \tau}d\tau + \int_{t_{-p+1}}^{t_{-p+2}} \beta(\tau)\frac{\partial x}{\partial \tau}d\tau + \ldots + \int_{t_0}^{t} \beta(\tau)\frac{\partial x}{\partial \tau}d\tau = \int_{t_{-p}}^{t} \beta(\tau)F(x,\tau)d\tau .$$

After the same term $\beta(t_i)x(t_i), i = -p+1, -p+2, \ldots, 0$ was eliminated, we have

$$\beta(t)x(t)-\beta(t_{-p})x(t_{-p})-\sum_{i=-p}^{0}[\beta(t_{i+1})-\beta(t_i)]x^m(t_i)-\int_{t_{-p}}^{t}\beta(\tau)F(x,\tau)d\tau=0 \quad \text{(B7)}$$

As a matter of convenience, we set $\beta_t \equiv \beta(t), \beta_0 \equiv \beta(t_0), x_t \equiv x(t), x_0 \equiv x(t_0)$; the following text uses similar notations. Then, Eq. (B7) can be expressed as:

$$\beta_t x_t - \beta_{-p}x_{-p} - \sum_{i=-p}^{0} x_i^m(\beta_{i+1}-\beta_i) - \int_{t_{-p}}^{t}\beta(\tau)F(x,\tau)d\tau = 0 \qquad \text{(B8)}$$

Setting $x_{-p} \equiv x_{-p-1}^m, \beta_{-p-1}=0$, the Eq. (B8) can be written as:

$$x_t = \frac{1}{\beta_t}\sum_{i=-p-1}^{0} x_i^m(\beta_{i+1}-\beta_i) + \frac{1}{\beta_t}\int_{t_{-p}}^{t}\beta(\tau)F(x,\tau)d\tau = S_1 + S_2 \qquad \text{(B9)}$$

S_1 is called as a self-memory term and S_2 is called as an exogenous effect term.

For the convenience of calculations, the above self-memorization equation can be discretized. The differential by difference and the summation can replace the integration in Eq. (B9), and the mean of two values which are at adjoining times; i.e., $x_i^m \approx \frac{1}{2}(x_{i+1}+x_i) \equiv y_i$ can simply replace x_i^m.

Taking an equal time interval $\Delta t_i = t_{i+1} - t_i = 1$ and incorporating β_i and β_t, we can obtain a discretized self-memorization equation as follows:

$$x_t = \sum_{i=-p-1}^{-1}\alpha_i y_i + \sum_{i=-p}^{0}\theta_i F(x,i) \qquad \text{(B10)}$$

where F is the dynamic kernel of the self-memorization equation, $\alpha_i = \frac{(\beta_{i+1}-\beta_i)}{\beta_t}$; $\theta_i = \frac{\beta_i}{\beta_t}$.

Based on Eq. (B10), the above technique performed computations and the forecast can be called as a self-memorization principle.

REFERENCES

Ashok K, Guan Z, Yam agata T : Impact of the Indian Ocean Dipole on the decadal relationship between the Indian mon soon rainfall and ENSO, Geophys Res Let,28(23), 4499-4502, 2001.

Balmaseda M.A., Davey M.K. and Anderson D.L.T.: Decadal and seasonal dependence of ENSO prediction skill,J Clim.,8, 2705–2715, 1995.

Barber R.T. and Chavez F.P.: Biological consequences of E1Niño,Science,222,1203-1210, 1983.

Barnston A. G., et al.: Skill of real-time seasonal ENSO model predictions during 2002-2011,Bull. Amer. Meteor. Soc.,93, 631-651, 2012.

Belkin M. and P. Niyogi: Laplacian eigenmaps for dimensionality reduction and data representation,Netural Comput.,15,1373-1391, 2003.

Bjerknes J.: Atmsopheric telconnections from the equtorail Pacific,Mon. Wea. Rev.,97,163-172, 1969.

Cao H. X.: Self-memorization Equation in Atmospheric Motion,Science in China (Series B),36(7), 845-855, 1993.

Chen D., S. E. Zebiak, A. J. Busalacchi and M. A. Cane: An Improved Procedure for El Nirio Forecasting: Implications for Predictability,Science, 269, 1699-1702, 1995.

Chen X. D., Xia J., Xu Q.: Differential Hydrological Grey Model(DHGM) with self-memory function and its application to flood forecasting,Sci China Tech Sci.,52,1039–1049, 2009.

Chou J.: The problem of utilizing past data in numerical weather forecasting,Sci. China, 6, 635-644, 1974 (in Chinese).

Clarke A. J. and S. Van Gorder: Improving El Niño prediction using a space-time integration of Indo-Pacific winds and equatorial Pacific upper ocean heat content,Geophys. Res. Lett.,30,1399. doi:10.1029/2002GL016673, 2003.

Delecluse P., Davey M., Kitamura Y., Philander S., Suarez M., Bengtsson L.: TOGA review paper: coupled general circulation modeling of the tropical Pacific,J Geophys Res,103,14357–14373, 1998.

Davey M., Huddleston M., Sperber K.R., et al.: A study of coupled model climatology and variability in tropical ocean regions,Clim. Dyn.,18,403–420, 2002.

Dommenget and Latif: A Cautionary Note on the Interpretation of EOFs, Journal of Climate,15(2),216–225, 2002.

Drosdowsky W.: Statistical prediction of ENSO (Niño 3) using sub-surface temperature data,Geophys. Res.Lett., 33 , L03710. doi:10.1029/2005GL024866, 2006.

Feng G. L., Cao H. X., Gao X. Q., et al.: Prediction of precipitation during summer monsoon with

Ocean Sci. Discuss., https://doi.org/10.5194/os-2017-78
Manuscript under review for journal Ocean Sci.
Discussion started: 7 November 2017

self-memorial model,Adv Atmos Sci.,18 ,701–709, 2001.

Fraedrich K.: Estimating weather and climate predictability on attractors,J .A tmos.Sci.,44,7 22-728, 1987.

Glantz MH, Katz RW, Nicholls N (eds): Teleconnections linking worldwide climate anomalies, 74pp,Cambridge University Press, Cambrige, UK, 1991.

Gu X. Q.: A spectral model based on atmospheric self_memorization principle,Chinese Science Bulletin,43(20),1692-1702 , 1998.

Hong M., Zhang R.andMa C. C.et al.: A Non-Linear Dynamical–Statistical Model for Reconstruction of the Air–Sea Element Fields in the Tropical Pacific Ocean,Atmosphere-Ocean, doi: 10.1080/07055900.2014.908765, 2014.

Hu, T.S., K.C. Lam, and S.T. Ng: River flow time series prediction with a range-dependent neural network,Hydrol. Sci. J., 46, 729–745, 2001.

Huang. J., Y. Yi, S. Wang, et al.: An analogue-dynamical long-range numerical weather prediction system incorporating historical evolution,Quart J Roy Meteor Soc, 119(511),547-565, 1993.

Huang J. P. and Yi Y. H.: A Non-linear Dynamic System Reconstructing of Actual data,Science in China,3 (3),331-336 , 1991.

James A. Carton and Benjamin S. Giese: A Reanalysis of Ocean Climate Using Simple Ocean Data Assimilation (SODA),Monthly Weather Review,136(8),2999-3011 , 2008.

Jin E. K.，James L. K.，Wang B.，et a1.: Current status of ENSO prediction skill in coupled ocean-atmosphere models,Climate Dyn,31, 647-664, 2008.

Johnson S.D., Battisit D.S. andSarachik E. S.: Empirically Derived Markov Models and Prediction of Tropical Pacific Sea SurfaceTemperature Anomalies, Journal of Climate,13,3-17, 2000.

Kalnay E., Kanamitsu M. and Kistler R.: The NCEP/NCAR 40-year reanalysisproject, Bull. Amer. Meteor. Soc.,77,437-470 , 1996.

Liao D., Zhou Y.H. and Liao X.H.: Modulation of the SSTA Decadal Variation on ENSO Events amd Relationships of SSTA with LOD, SOI, etc.,Acta Astronomica Sinica,48(1),36-47 , 2007.

Liebmann B. and C.A. Smith: Description of a Complete (Interpolated) Outgoing Longwave Radiation Dataset,Bulletin of the American Meteorological Society,77,1275-1277, 1996.

Li L. P., Wang P. X., He J. H. and Wang D. X.: Analysis of interdecadal and interannual Characteristics of the Tropical western Pacific Warm Pool heat status,Journal of Tropical

Meteorology,20(5),472-482 , 2004.

Luo, J.-J., S. Masson, S. Behera, S. Shingu, andT. Yamagata: Seasonal climate predictabilityin a coupled OAGCM using a different approach forensemble forecasts,J. Climate, 18,4474–4497, 2005.

Mechoso C.R., Robertson A.W., Barth N., et al.: The seasonal cycle over the tropical Pacific in coupled atmosphere–ocean generalcirculation models,Mon Weather Rev,123,2825–2838, 1995.

Molteni F., et al.: ECMWF seasonal forecast system3,CLIVAR Exch,43,7-9, 2007.

Moore A. M., Zavala-Garay J. and Tang Y., et al.: Optimal forcing patterns for coupled models of ENSO,J Climate,19,4683-4699 , 2006.

Neelin J.D., Latif M. and Allaart M.A.F.: Tropical air-sea interaction in general circulation models,Clim Dyn.,7,73–104, 1992.

Palmer T. N., Alessandri A. and Andersen U., et al.: Development of a European multi-model ensemble system forseasonal to interannual prediction (DEMETER),Bull Amer Met Soc.,85,853-872 , 2004.

Panofsky H.A., Brier G.W.: Some applications of statistics tometeorology, Pennsylvania State University Press, Pennsylvania , 1968.

Rasmusson E.M. and Carpenter T.H.: Variations in tropical seasurface temperature and surface wind fields associated with the Southern Oscillation/E1 Ni ño,Mon Weather Rev.,10, 354-384, 1982.

Reynolds, R. W., N. A. Rayner, T. M. Smith, D. C.Stokes, and W. Wang: An improved in situand satellite SST analysis for climate,J. Climate,15,1609–1625, 2002.

Saha S., Nadiga C. and Thiaw J., et al.: The NCEP climate forecast system,Journal of Climate,19 ,3483-3517 , 2006.

Sa ji N. H., Goswami B. N., V. inayachandran P. N., et al.: A dipole mode in the tropical Indian Ocean,Nature, 401(6751),360-363, 1999.

Takens, F.: Detecting strange attractors in fluid turbulence,Lecture Notes in Mathematics,898(2),361-381 , 1981.

Tetko, I. V., Livingstone, D. J., Luik, A. I.: Neural network studies. 1. Comparison of Overfitting and Overtraining, J. Chem. Inf. Comput. Sci.,35 (5), 826–833 , 1995.

Timmermann A., Voss H. U. and Pasmanter R.: Empirical Dynamical System Modeling of ENSO Using Nonlinear Inverse Techniques, Journal of Physical Oceanography, 31,1579-1598 , 2001.

Tomita, T., and T. Yasunari: Role of the northeast winter monsoon on the biennial oscillation of the

Ocean Sci. Discuss., https://doi.org/10.5194/os-2017-78
Manuscript under review for journal Ocean Sci.
Discussion started: 7 November 2017

ENSO/monsoon system,J. Meteor. Soc. Japan, 74,399–413 , 1996.

Trenberth, E.   K., et al.: Progress during TOGA in understanding and modeling global teleconnections associated with tropical sea surface temperatures,J. Geophys. Res., 107, C7, 14291-14324,1998.

Wang B., Wu R., Lukas R.: Roles of western North Pacific wind variation in thermocline adjustment and ENSO phase transition,J Meteor Soc Japan,77,1-16,1999a.

Wang B.，Lee J. Y.，Shukla J.，et al.: Advance and prospectus of seasonal prediction：assessment of the APCC / CIiPAS 14-Model Ensemble Retrospective Seasonal Prediction(1980—2004),Climate Dyn.,33(1),93-117 , 2009.

Wang C., Weisberg R. H. and Virmani J. I.: Western Pacific interannual variability associated with the El Niño-Southern Oscillation,J Geophy Res.,104,5131-5149, 1999b.

Wang, L., W. Chen, and R. H. Huang: Interdecadal modulation of PDO on the impact of ENSO on the eastAsian winter monsoon,Geophys. Res. Lett., 35, L20702, doi:10.1029/2008GL035287, 2008.

Wang L.: Intelligent Optimization Algorithms and Its Application, pp. 23-24, Tsinghua University Press, Chendu, 2001.

Wang W., Su J. Y., Hou B. W. et al.: Dynamic prediction of building subsidence deformation with data-based mechanistic self-memory model,Chinese Science Bulletin,57(26),3430-3435, 2012.

Webster P. J., Moore A. M., Loschnigg J. P., et al.: Coupled ocean-atmosphere dynamics in the Indian Ocean during 1997- 98, Nature, 401(6751),356-360, 1999.

Weinberger K. Q. and L. Saul: Unsupervised learning of image manifolds by semidefinite programming,Int. J. Comput. Vision.,70, 77-90, 2006.

Xu J. J. and Wang D. X.: Diagnosis of interannual and interdecadal variation in SST over Indian-Pacific Ocean and numerical simuation of their effect on Asian summer monsoon,Acta Oceanologica Sinica,22(3),34-43 , 2000.

Yang, S., K. M. Lau, and K. M. Kim: Variations of the East Asian jet stream and Asian-Pacific-American winter climate anomalies, J. Climate, 15,306–325 , 2002.

Yim SY, Wang B, Kwon M: Interdecadal change of the controlling mechanisms for East Asian early summer rainfall variation around the mid-1990s.ClimDyn., 42,1325–1333, 2013.

Yim, S.-Y., B. Wang, W. Xing, M.-M.Lu: Prediction of Meiyu rainfall in Taiwan by multi-lead physicalempiricalmodels.Clim. Dyn., 44 (11-12), 3033-3042, doi:10.1007/s00382-014-2340-0, 2015.

Yoon, J., and S. W. Yeh: Influence of the Pacific Decadal Oscillation on the relationship between El

Ocean Sci. Discuss., https://doi.org/10.5194/os-2017-78
Manuscript under review for journal Ocean Sci.
Discussion started: 7 November 2017

Ni˜no and the northeast Asian summer monsoon, J. Climate,23, 4525–4537, 2010.

Yu H., J. Huang, and J. Chou: Improvement of Medium-Range Forecasts Using the Analogue-Dynamical Method,Mon. Wea. Rev., 142, 1570–1587, doi: http://dx.doi.org/10.1175/MWR-D-13-00250.1, 2014a.

Yu H., J. Huang, W. Li, and G. Feng: Development of the analogue-dynamical method for error correction of numerical forecasts,J. Meteor. Res., 28(5), 934–947, doi: 10.1007/s13351-014-4077-4 , 2014b.

Zhang R. and Hong M., et al.: Non-linear Dynamic Model Retrieval of Subtropical High Based on Empirical Orthogonal Function and Genetic Algorithm,Applied Mathematics and Mechanics,27(12),1645-1654, 2006.

Zhang R. and Hong M.,et al.: Retrieval of the non-linear dynamic forecast model of El Nino/La Nina index based on the genetic algorithm optimization. Chinese Journal of Geophysics,51(5),1354-1362, 2008.

Zhang R. H., Zhou G. Q. and Chao J. P.: ENSO Dynamics and Its Prediction,Chinese Journal of Atmospheric Sciences,27(4) ,674-688, 2003.

Zhang, R. H., A. Sumi, and M. Kimoto: Impact of El Ni˜noon the East Asian monsoon: A diagnostic study of the '86/87 and '91/92 events,J. Meteor. Soc. Japan, 74, 49–62, 1996.

Zhao J. H., Liu X. Y. and Jiang H. Y., et al.: Characteristics of Sea Surface Height in Tropical Pacific and its relationship with ENSO events,Meteorological and Environmental Sciences, 35(2),33-39, 2012.

Zhou, L.-T., and R. G. Wu: Respective impacts of the East Asian winter monsoon and ENSO on winter rainfall in China,J. Geophys. Res.,115, doi: 10.1029/2009JD012502, 2010.

Ocean Sci. Discuss., https://doi.org/10.5194/os-2017-78
Manuscript under review for journal Ocean Sci.
Discussion started: 7 November 2017

List of Figures:

Table captions:

Figure:

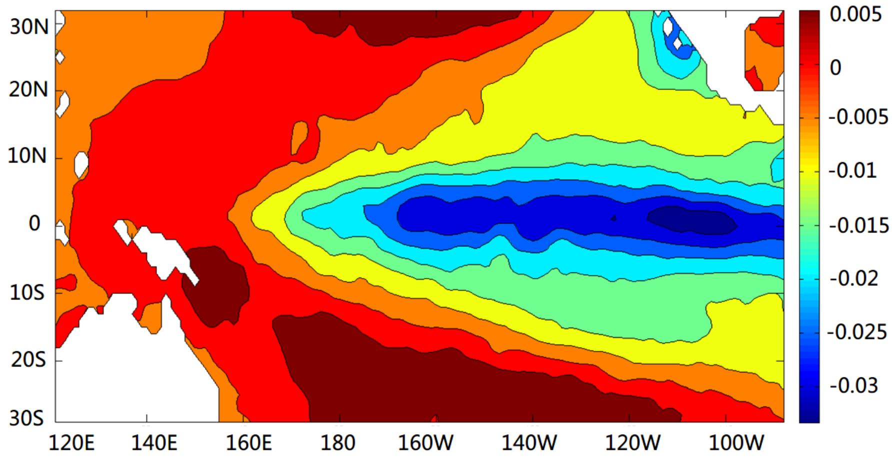
30N
20N
10N
0
10S
20S
30S
120E
140E
160E
180
160W
140W
120W
100W
0.005
0
-0.005
-0.01
-0.015
-0.02
-0.025
-0.03

(a)

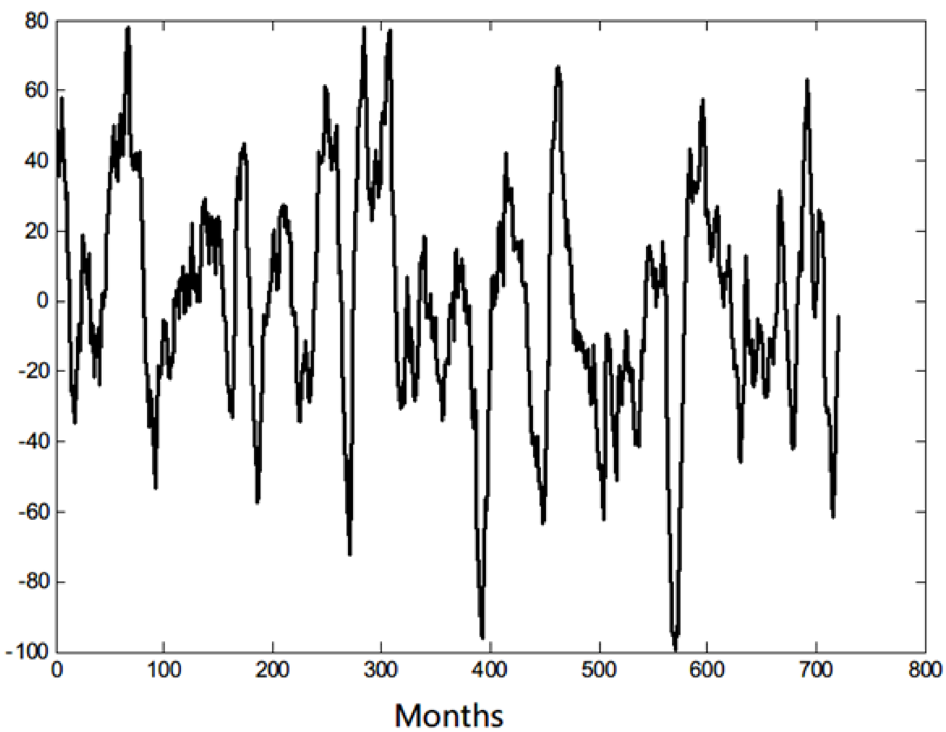
80
60
40
20
0
-20
-40
-60
-80
-100
0
100
200
300
400
500
600
700
800
Months

(b)

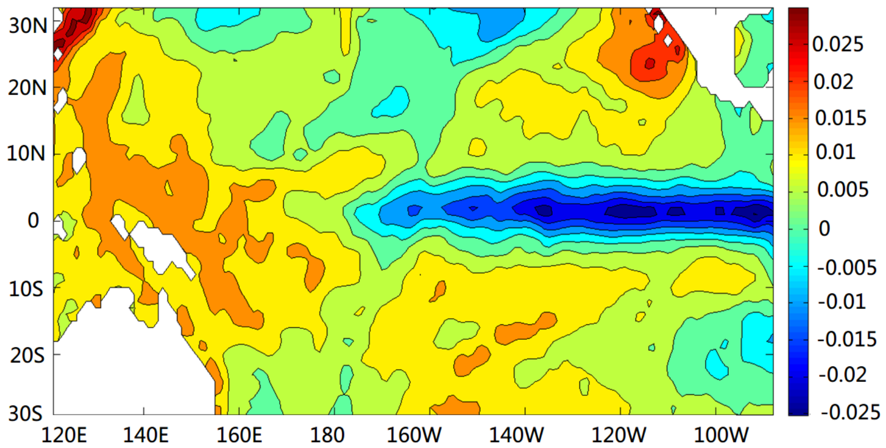

(c)

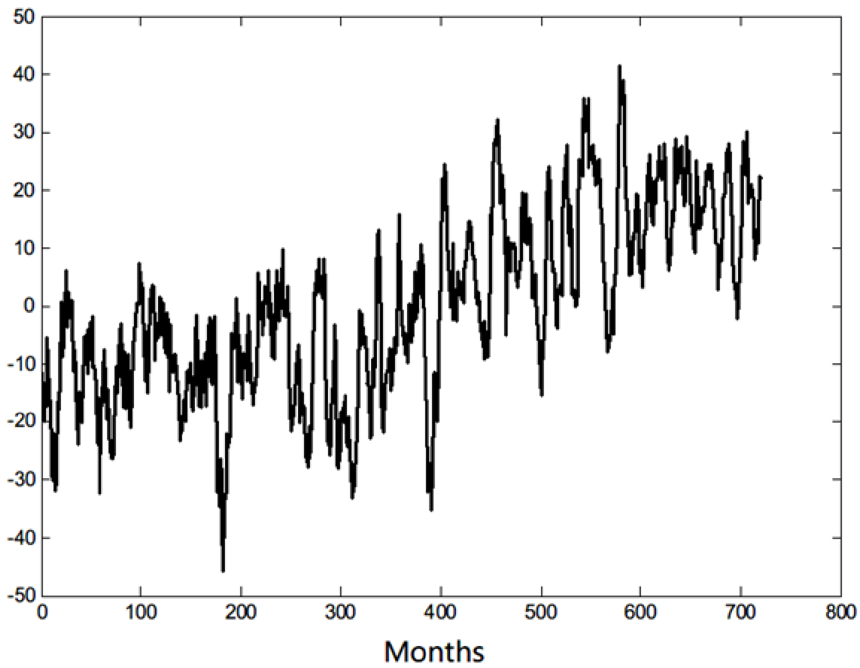

(d)

Fig. 1 (a, c) First and second modes of the EOF deconstruction of the SSTA field, and (b, d) the corresponding PC time series.

Ocean Sci. Discuss., https://doi.org/10.5194/os-2017-78
Manuscript under review for journal Ocean Sci.
Discussion started: 7 November 2017

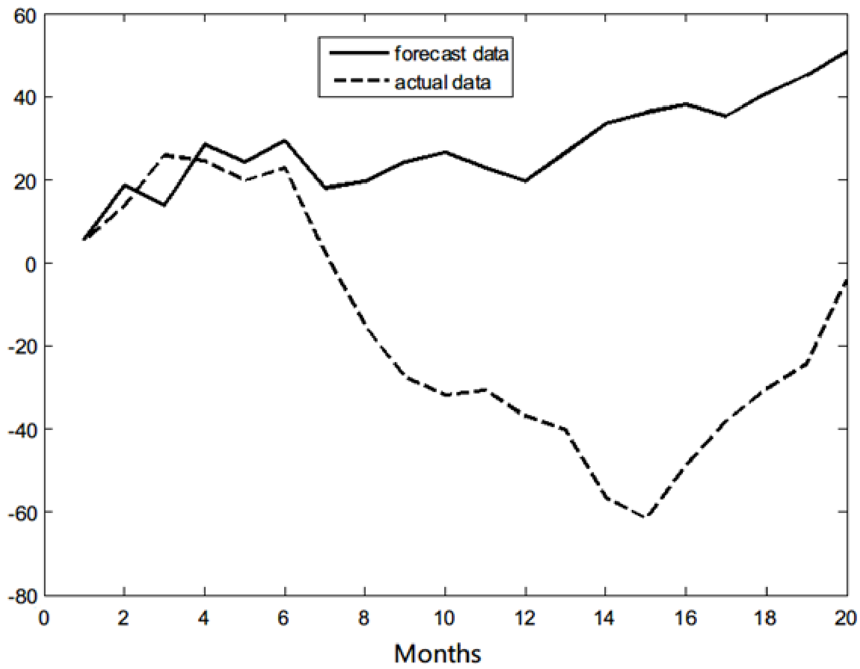

961

962 (a)

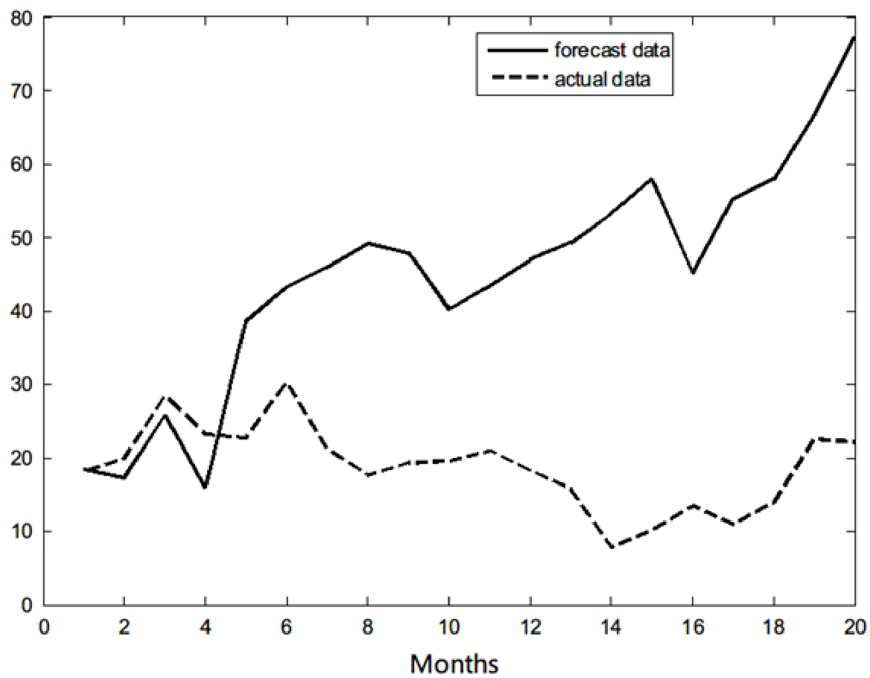

963

Ocean Sci. Discuss., https://doi.org/10.5194/os-2017-78
Manuscript under review for journal Ocean Sci.
Discussion started: 7 November 2017

(b)

Fig.2 Forecast results of the first time coefficient series T_1 (a) and the second time coefficient series T_2 (b)of the SSTA field by the original model

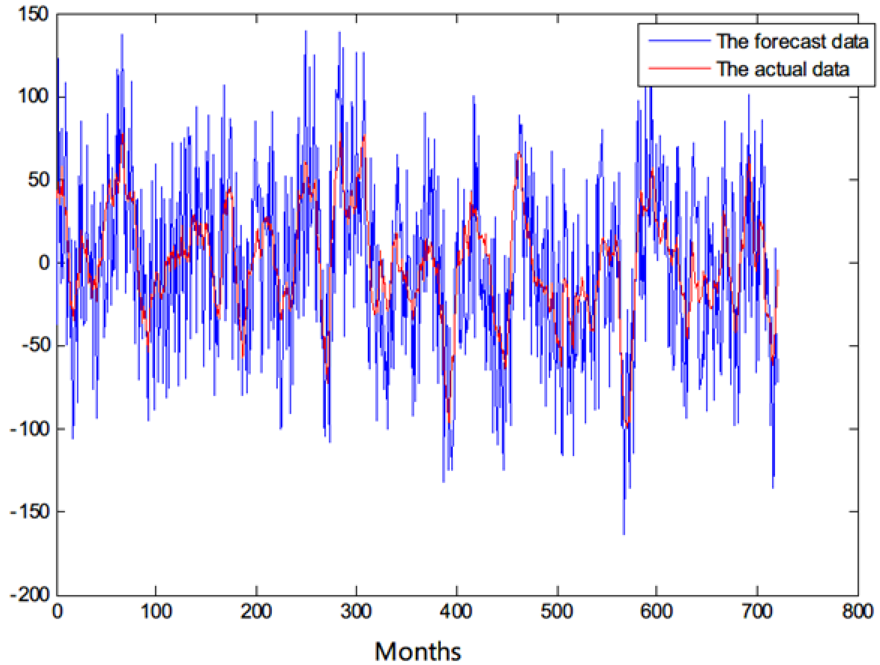
The forecast data
The actual data
150
100
50
0
-50
-100
-150
-200
0
100
200
300
400
500
600
700
800
Months

(a)

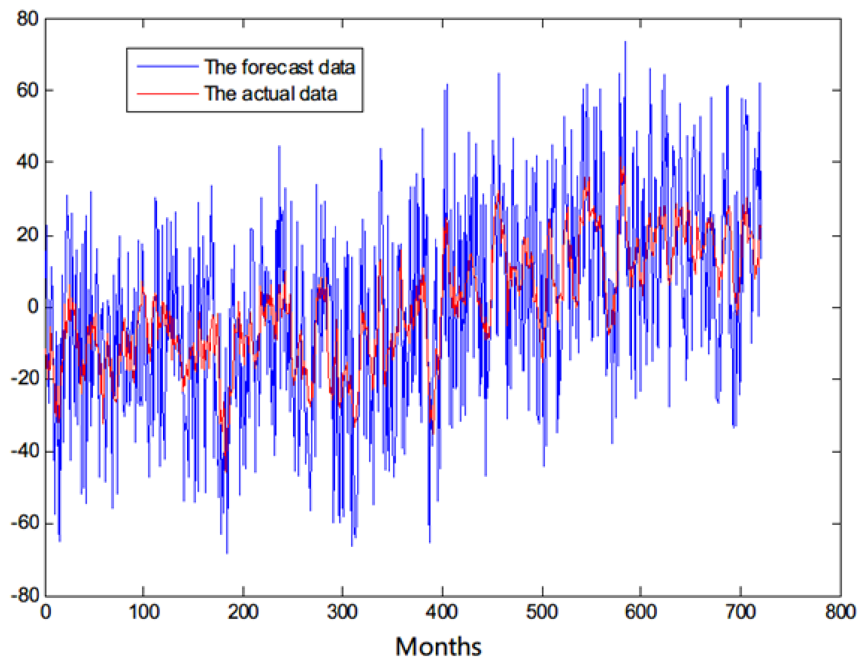
The forecast data
The actual data
80
60
40
20
0
-20
-40
-60
-80
0
100
200
300
400
500
600
700
800
Months

Ocean Sci. Discuss., https://doi.org/10.5194/os-2017-78
Manuscript under review for journal Ocean Sci.
Discussion started: 7 November 2017

(b)

Fig.3The cross-validated retroactive hindcast results of the first time coefficient series T_1 (a)and the second time coefficient series T_2 (b)of the SSTA field by the original model

Ocean Sci. Discuss., https://doi.org/10.5194/os-2017-78
Manuscript under review for journal Ocean Sci.
Discussion started: 7 November 2017

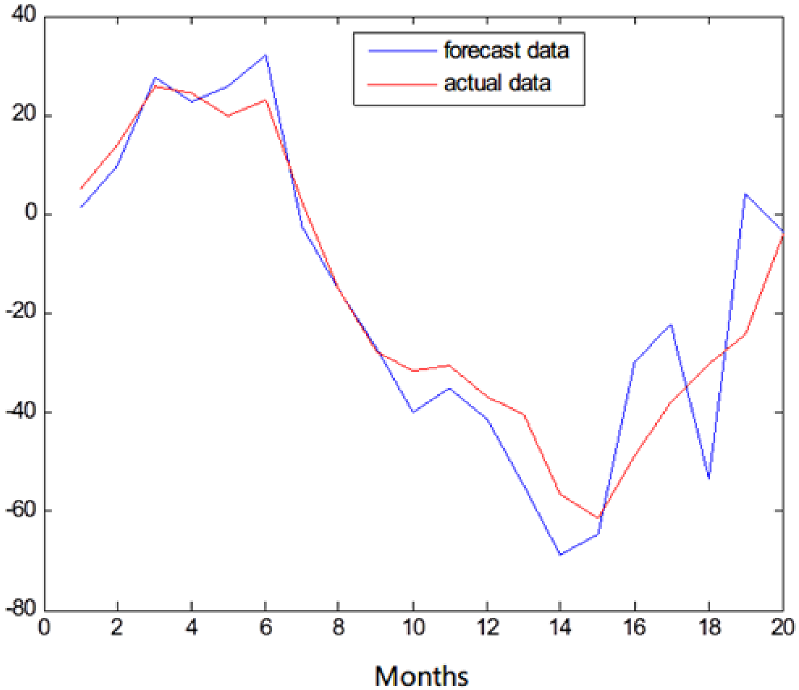

993

994 (a)

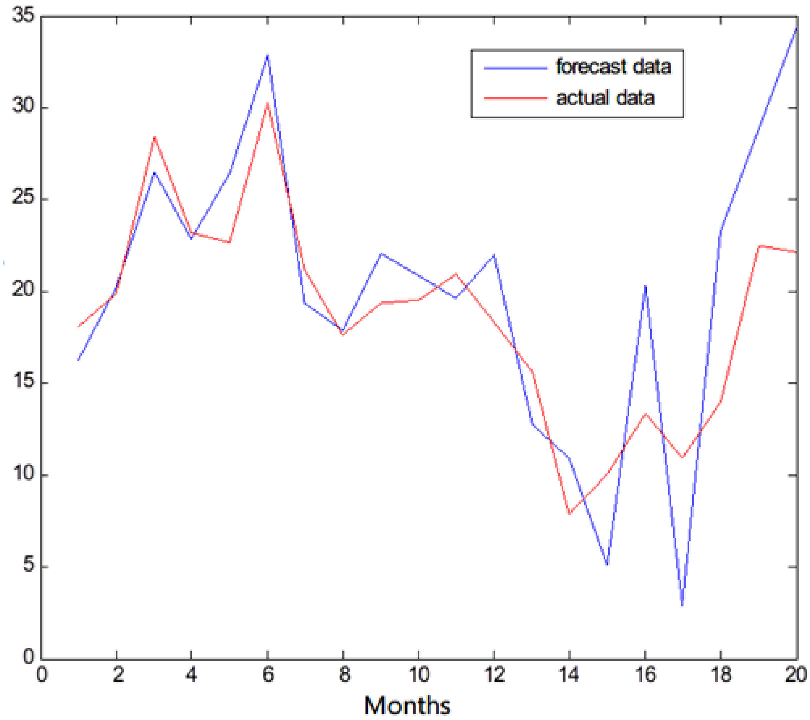

(b)

Fig. 4. Long-term step-by-step forecast results of the first time coefficient series T_1 (a)and the second time coefficient series T_2 (b)of the SSTA field by the improved model

Ocean Sci. Discuss., https://doi.org/10.5194/os-2017-78
Manuscript under review for journal Ocean Sci.
Discussion started: 7 November 2017

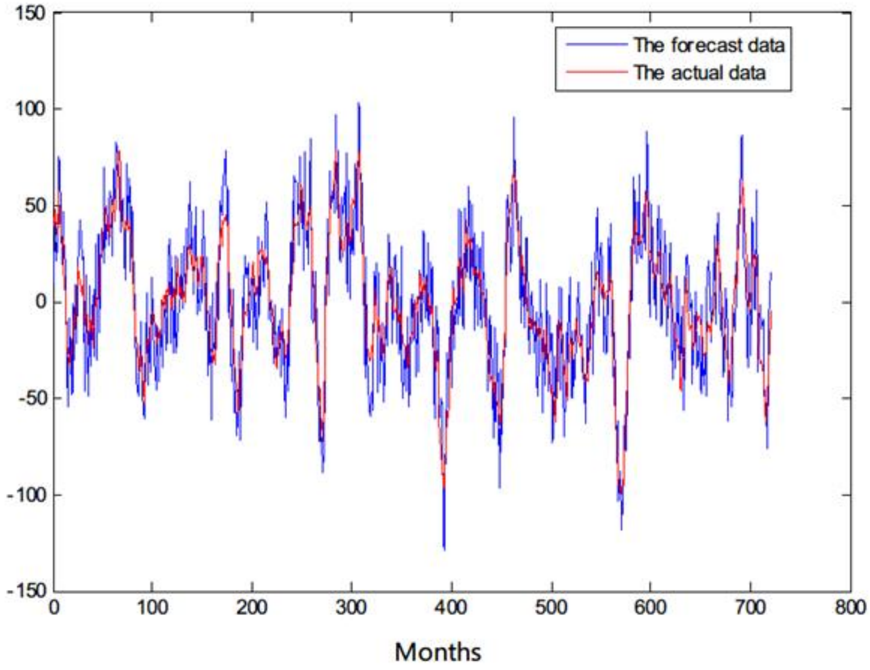

(a)

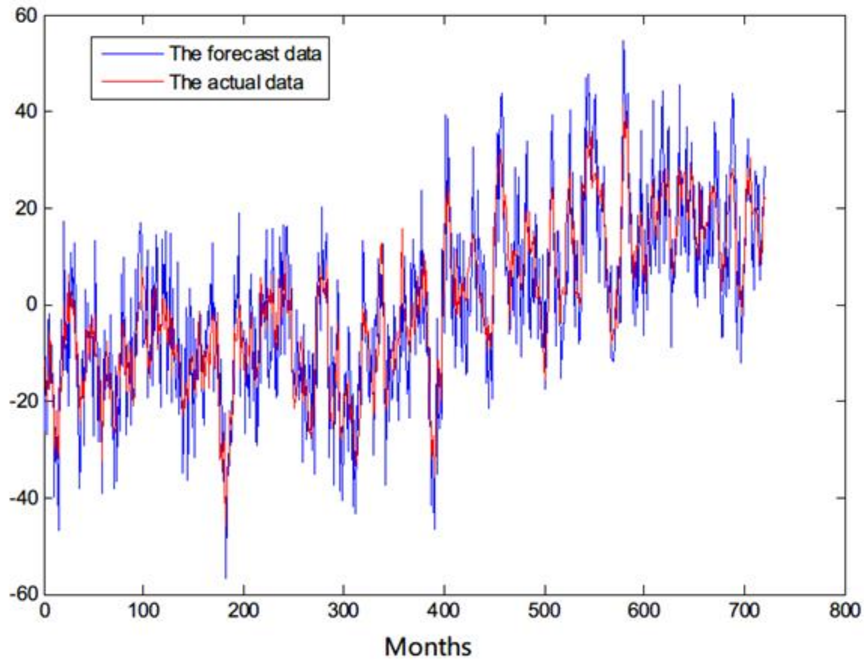

Ocean Sci. Discuss., https://doi.org/10.5194/os-2017-78
Manuscript under review for journal Ocean Sci.
Discussion started: 7 November 2017

Ocean Science Discussions
Open Access

(b)

Fig. 5. The cross-validated retroactive hindcast results of the first time coefficient series T_1 (a)and the second time coefficient series T_2 (b)of the SSTA field by the improved model

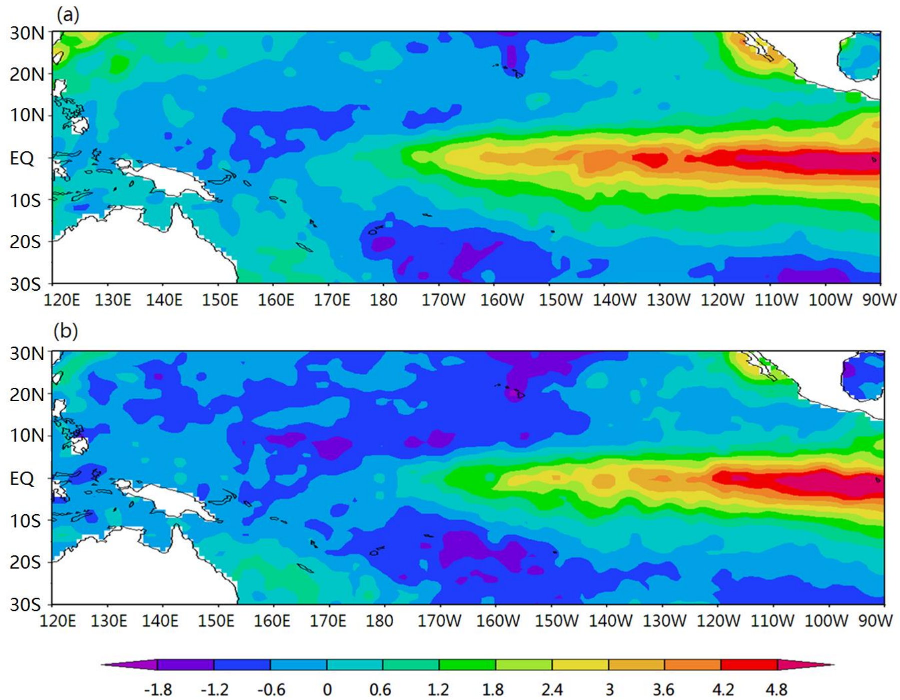

Fig.6. The forecast SSTA field(a) and the actual SSTA field (b)of an El Niño event (Dec.1997)

Ocean Sci. Discuss., https://doi.org/10.5194/os-2017-78
Manuscript under review for journal Ocean Sci.
Discussion started: 7 November 2017

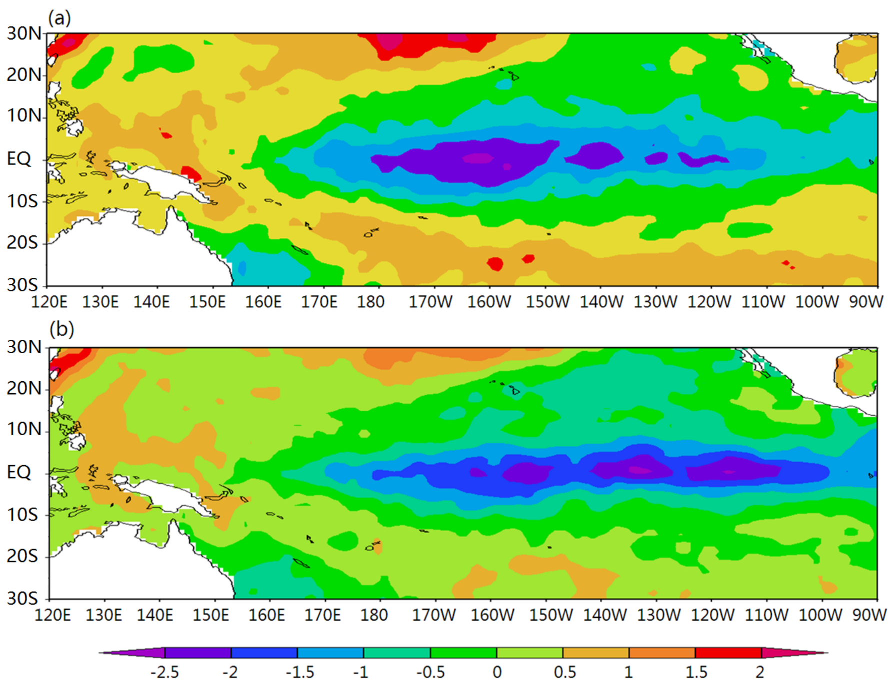

Fig.7. The forecast SSTA field(a) and the actual SSTA field (b)of a La Niña event (Dec.1999)

Ocean Sci. Discuss., https://doi.org/10.5194/os-2017-78
Manuscript under review for journal Ocean Sci.
Discussion started: 7 November 2017

1035

1036

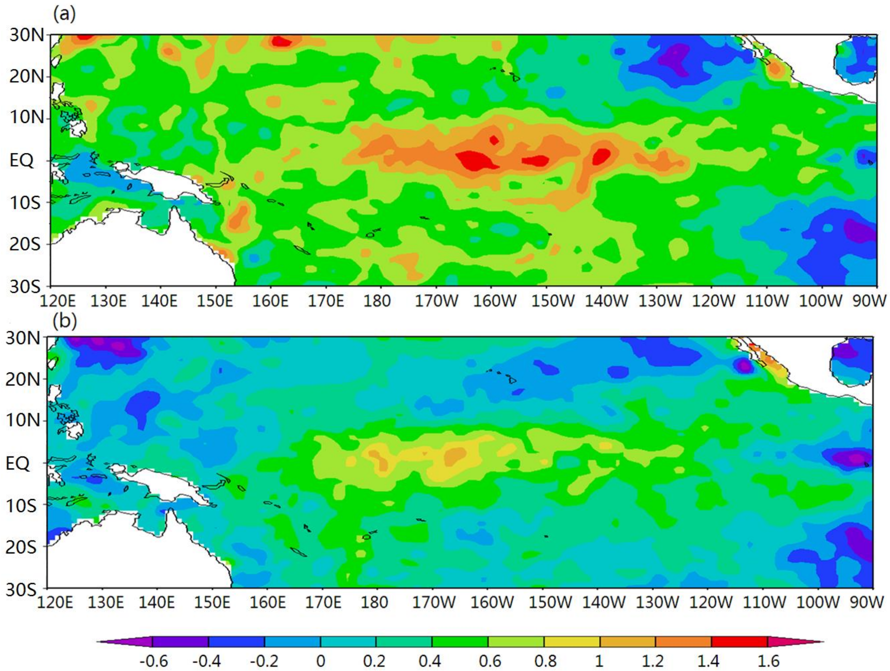

1037

1038 Fig.8. The forecast SSTA field(a) and the actual SSTA field (b)of neutral event (Nov.2002)

1039

Ocean Sci. Discuss., https://doi.org/10.5194/os-2017-78
Manuscript under review for journal Ocean Sci.
Discussion started: 7 November 2017

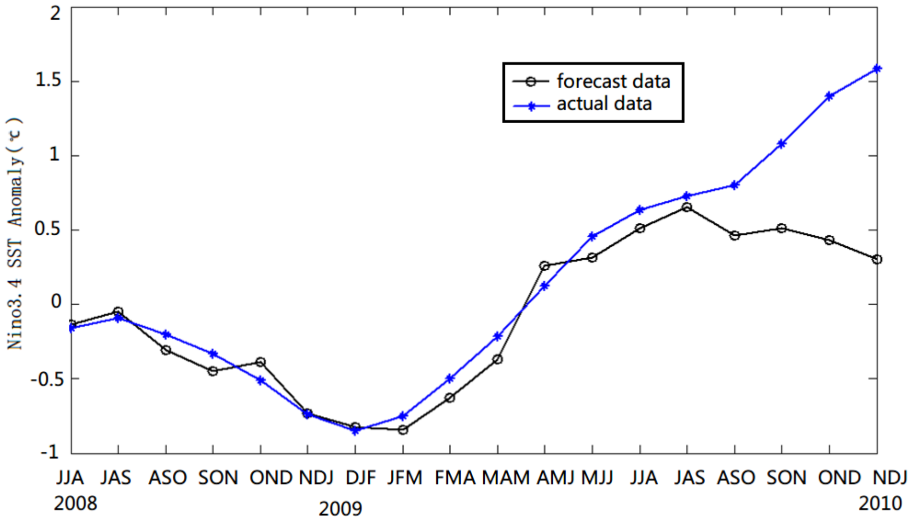

Fig.9. The improved dynamical-statistical model prediction of the ENSO index

Ocean Sci. Discuss., https://doi.org/10.5194/os-2017-78
Manuscript under review for journal Ocean Sci.
Discussion started: 7 November 2017

Ocean Science
Discussions
Open Access

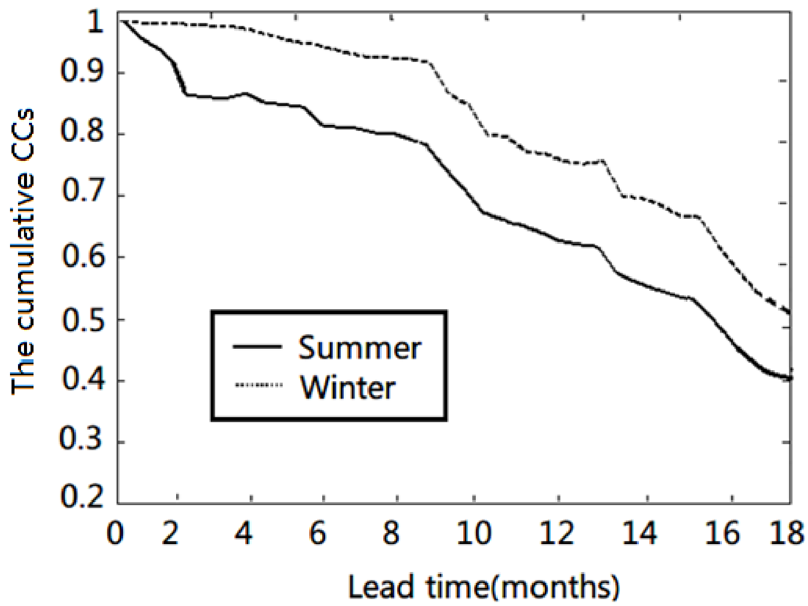

(a)

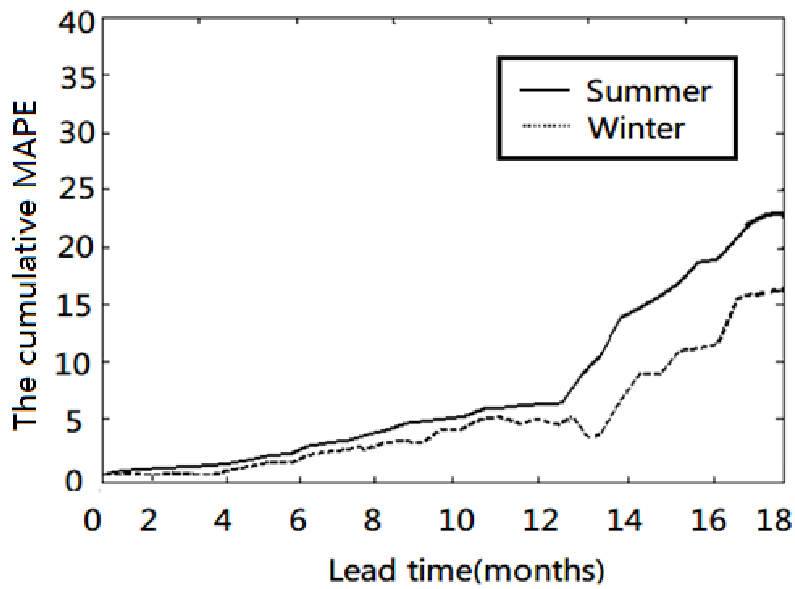

(b)

Fig.10. The cumulative correlation coefficients(CCs) (a) and cumulative mean absolute percentage error(MAPE) (b) changing with time of different lead times

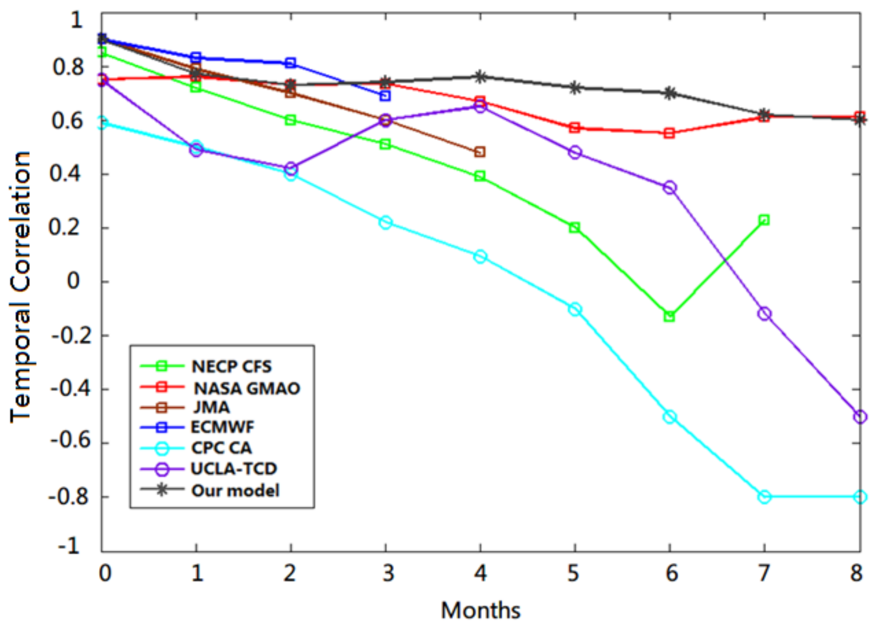

Fig. 11. Temporal correlation between model forecasts and observations for all seasons combined, as a function of lead time. Each line highlights one model.

Ocean Sci. Discuss., https://doi.org/10.5194/os-2017-78
Manuscript under review for journal Ocean Sci.
Discussion started: 7 November 2017

Ocean Science
Discussions
Open Access

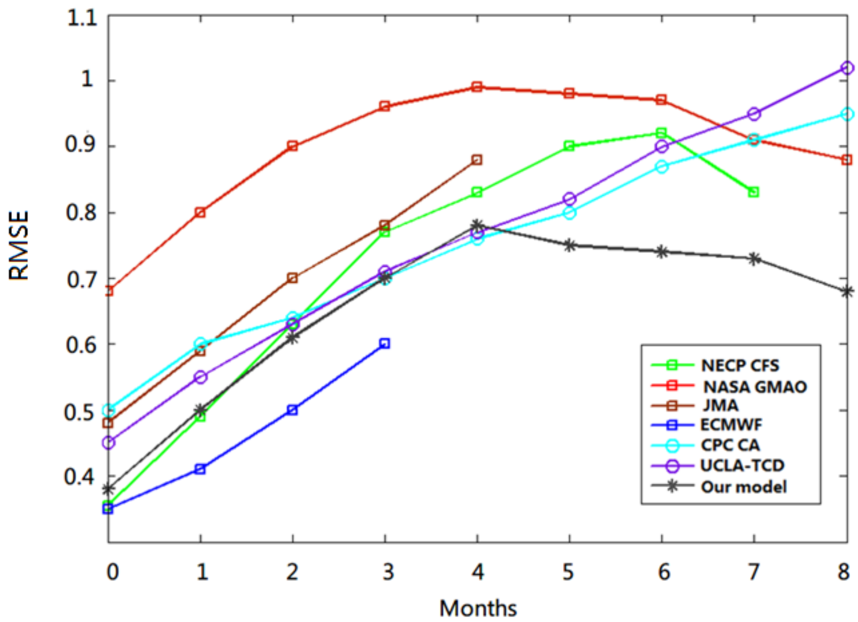

Fig . 12. RMSE in standardized units, as a function of lead time for all seasons combined. Each line highlights one model.

Ocean Sci. Discuss., https://doi.org/10.5194/os-2017-78
Manuscript under review for journal Ocean Sci.
Discussion started: 7 November 2017

Table:

Table1. The forecast results of the models of different variables

The model	The forecast skill of 60 cross-validated retroactive hindcasts experiments of the ENSO index for all seasons combined at lead times of 8 months	
	the temporal correlation	the root mean square error
One variable（T_1）	0.5051	0.8075
Two variables（T_1, T_2）	0.5613	0.7679
Three variables（T_1, T_2, SOI）	0.6027	0.7275
Four variables（$T_1, T_2, SOI, EAWMI$）	0.6344	0.6728
Five variables（$T_1, T_2, SOI, EAWMI, u_1$）	0.5923	0.7344
Six variables（$T_1, T_2, SOI, EAWMI, u_1, PNA$）	0.5528	0.7806

Ocean Sci. Discuss., https://doi.org/10.5194/os-2017-78
Manuscript under review for journal Ocean Sci.
Discussion started: 7 November 2017

Table2. The correlation coefficient(CC) and Mean absolute percentage error(MAPE) of long-term fitting test when the retrospective order p is different

p		4	5	6	7	8	9	10
The forecast results of long-term fitting test	CC	0.75	0.73	0.81	0.74	0.70	0.72	0.68
	MAPE	18.42%	19.36%	14.56%	20.39%	25.31%	24.18%	27.33%
p		11	12	13	14	15	16	
The forecast results of long-term fitting test	CC	0.68	0.70	0.65	0.62	0.60	0.62	
	MAPE	28.10%	26.58%	30.91%	33.14%	34.97%	33.56%	

Ocean Sci. Discuss., https://doi.org/10.5194/os-2017-78
Manuscript under review for journal Ocean Sci.
Discussion started: 7 November 2017

Table3. The forecast results of T_1 and T_2 in different examples within 6 and 12 months

Forecast events	The results within 6-months		The results within 12-months	
	CC	MAPE	CC	MAPE
The average of 18 El Niño examples of T_1	0.824	8.45%	0.719	12.67%
The average of 22 La Niña examples of T_1	0.846	7.68%	0.740	11.28%
The average of 20 Neutral examples of T_1	0.885	6.23%	0.789	9.85%
The average of total 60 examples of T_1	0.850	7.41%	0.748	10.95%
The average of 18 El Niño examples of T_2	0.811	8.79%	0.703	13.28%
The average of 22 La Niña examples of T_2	0.833	7.35%	0.731	11.96%
The average of 20 Neutral examples of T_2	0.896	6.68%	0.795	10.08%
The average of total 60 examples of T_2	0.842	7.64%	0.740	11.71%

Table. 4. Temporal correlation(CC) and the mean absolute percentage error (MAPE) between model forecasts and observations within 12 months for Nov–Jan, Dec–Feb, and Jan–Mar as lead time.of winter and for May-July, June-August and July-Sep. as lead time of summer.

Forecast events	Lead time of all seasons combined		Lead time of summer (MJJ-JJA-JAS)		Lead time of winter (NDJ-DJF-JFM)	
	CC	MAPE	CC	MAPE	CC	MAPE
The average of 18 El Niño examples	0.604	9.70%	0.569	10.33%	0.677	8.02%
The average of 22 La Niña examples	0.625	8.97%	0.581	9.82%	0.695	7.83%
The average of 20 Neutral examples	0.798	5.96%	0.752	6.86%	0.844	4.60%
The average of total 60 examples	0.712	7.62%	0.633	8.51%	0.776	6.52%

Ocean Sci. Discuss., https://doi.org/10.5194/os-2017-78
Manuscript under review for journal Ocean Sci.
Discussion started: 7 November 2017

1161

1162 **Table5.** The correlation coefficients among four factors

Correlation coefficients	T_1	T_2	SOI	EAWMI
T_1		0.419	0.401	0.337
T_2	0.419		0.424	0.356
SOI	0.401	0.424		0.408
EAWMI	0.337	0.356	0.408	

1163

1164